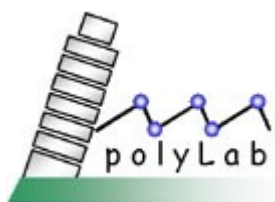


Present and Future Regimes and Applications of Laser-Plasma Ion Acceleration

Andrea Macchi

*polyLAB, CNR-INFM, Pisa
Dipartimento di Fisica "Enrico Fermi", Università di Pisa
and INFN, sezione di Pisa, Italy*



CNR- IPCF, Pisa, December 6, 2007

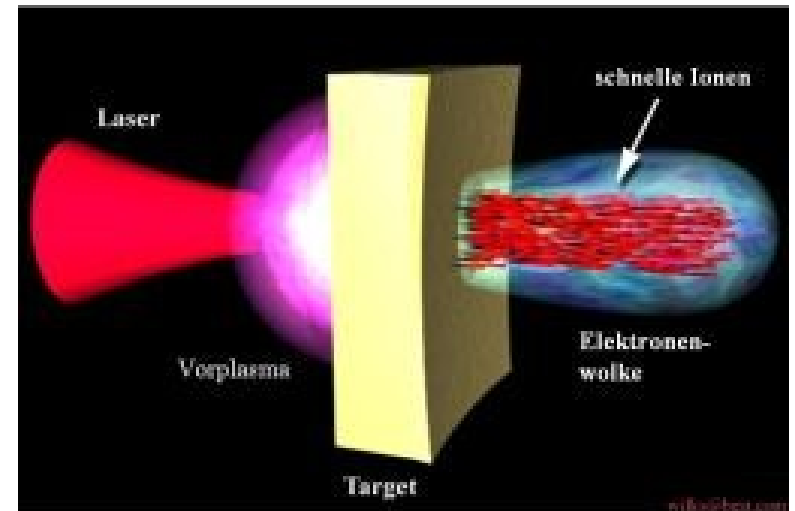
Outline

- The “new era” of laser acceleration of ions (mainly protons): their discovery and (foreseen) applications
- Present regimes (mainly Target Normal Sheath Acceleration)
- Future regimes (mainly Radiation Pressure Acceleration)
- A proposal: RPA with circularly polarized pulses
- Some (preliminary) suggestions for FLAME experiments

The discovery of MeV proton emission in superintense interaction with *metallic* targets

Reported in 2000
by three experimental groups

[Clark et al, PRL **84** (2000) 670;
Maksimchuk et al, *ibid.*, 4108;
Snavely et al, PRL **85** (2000) 2945 (*)]



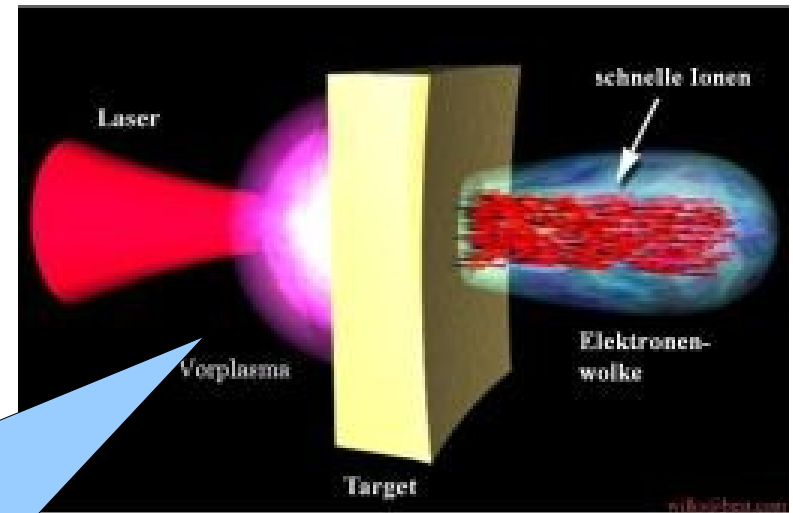
Remarkable properties
of the proton beam:

- **high number** (up to 10^{14})
- **good collimation**
- **ultra-low emittance** (4×10^{-3} mm mrad)
- maximum energy and efficiency observed (*):
58 MeV , 12% of laser energy
@ $I=3 \times 10^{20}$ W/cm²

The discovery of MeV proton emission in superintense interaction with *metallic* targets

Reported in 2000
by three experimental groups

[Clark et al, PRL **84** (2000) 670;
Maksimchuk et al, *ibid.*, 4108;
Snively et al, PRL **85** (2000) 2945 (*)]



Question: why protons
from *metallic* targets?

Answer: presence of a layer
of hydrocarbon or water
impurities on
the target surface

er (up to 10^{14})

tion

ttance (4×10^{-3} mm mrad)

gy and efficiency

of laser energy

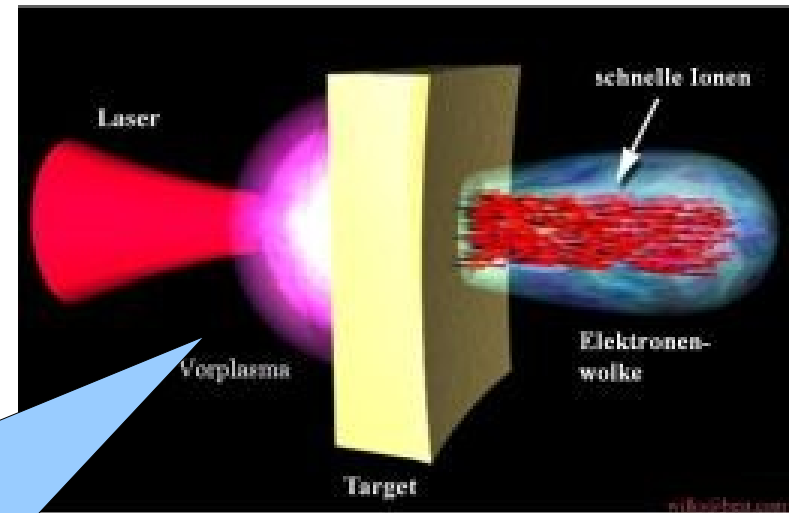
N/cm^2

Rem
of th

The discovery of MeV proton emission in superintense interaction with *metallic* targets

Reported in 2000
by three experimental groups

[Clark et al, PRL **84** (2000) 670;
Maksimchuk et al, *ibid.*, 4108;
Snavely et al, PRL **85** (2000) 2945 (*)]



More debated

question: are protons coming from the *front* or from the *rear* side?

i.e. what is the acceleration mechanism?

Intensity (up to 10^{14})

Wavelength

Spot size (4 x 10^{-3} mm mrad)

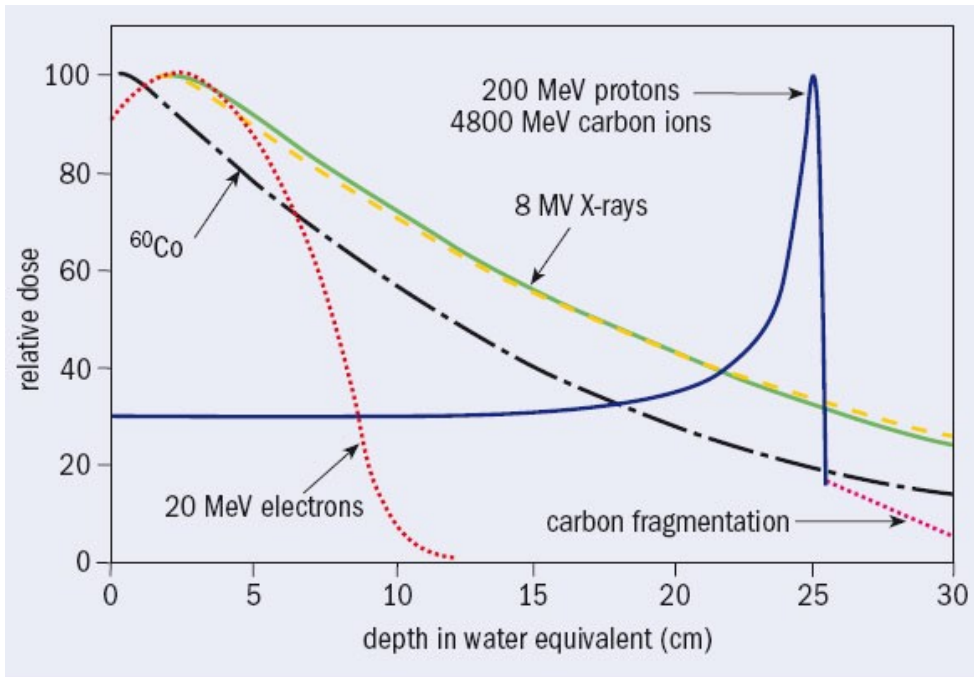
Energy and efficiency

Conversion of laser energy

W/cm²

Rem
of th

MeV protons (ions) are appealing for applications requiring localized energy deposition in matter



Sharp spatial maximum of deposited energy
(**Bragg peak**)

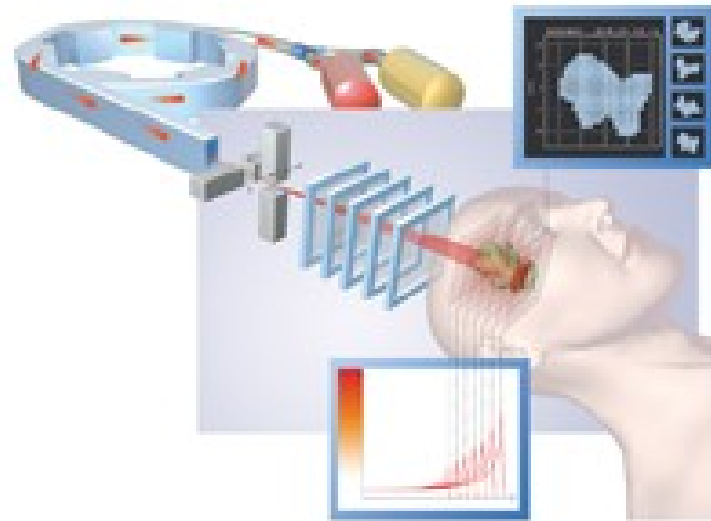
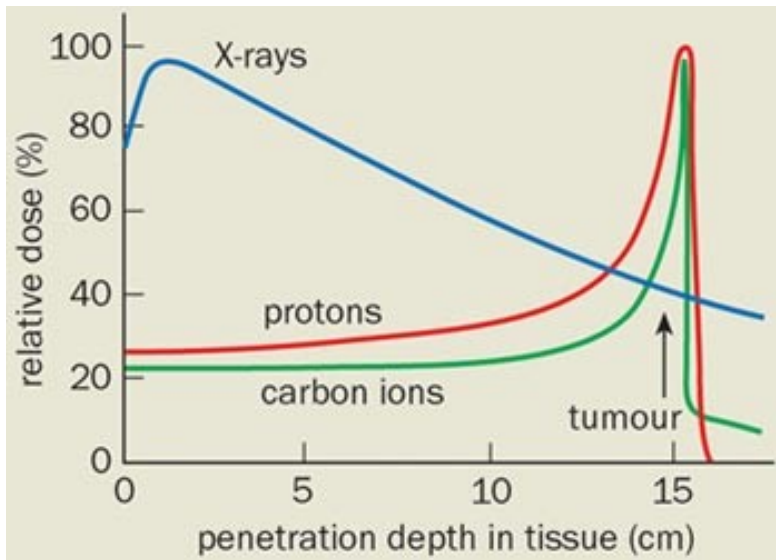
Peak location depends on energy

[U. Amaldi & G. Kraft, Rep. Prog. Phys. **68** (2005) 1861]

MeV protons (ions) are appealing for applications requiring localized energy deposition in matter

Medical Applications

ONCOLOGICAL HADRONTHERAPY



[K.Ledingham, Glasgow University, 2006]

If feasible with table-top, high repetition lasers, **cost can be reduced** with respect to an accelerator facility

Other foreseen application in medicine: **isotope production** (e.g. for Proton Emission Tomography)

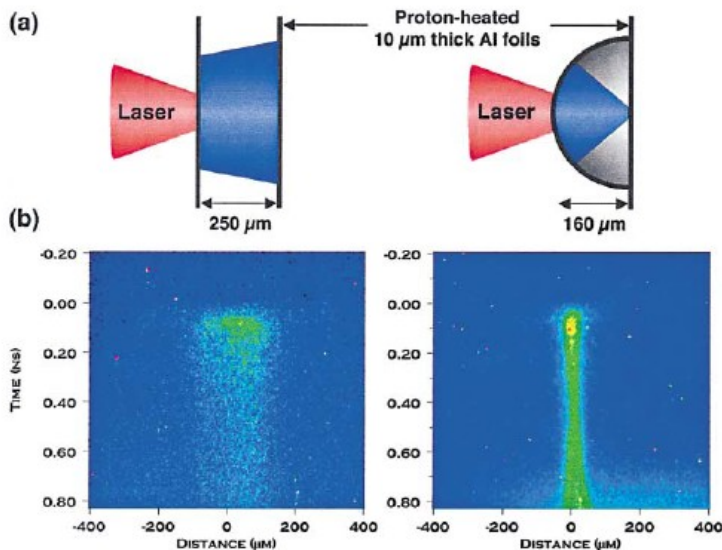
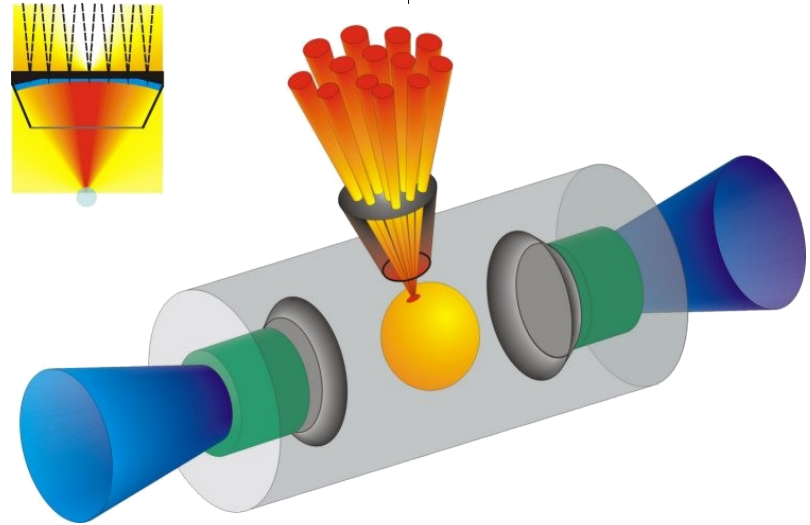
MeV protons (ions) are appealing for applications requiring localized energy deposition in matter

Inertial **C**onfinement **N**uclear **F**usion

FAST IGNITION

Protons can be used to create a “spark” in a pre-compressed ICF capsule achieving **isochoric burn** and **high energy gain**

[Roth et al, Phys. Rev. Lett. **86** (2001) 436;
Atzeni et al, Nuclear Fusion **42** (2002) L1;
Macchi et al, Nuclear Fusion **43** (2003) 362]



Geometrical focusing of laser-accelerated protons and localized **isochoric heating** has been demonstrated

[Patel et al, Phys. Rev. Lett. **91** (2003) 125004]

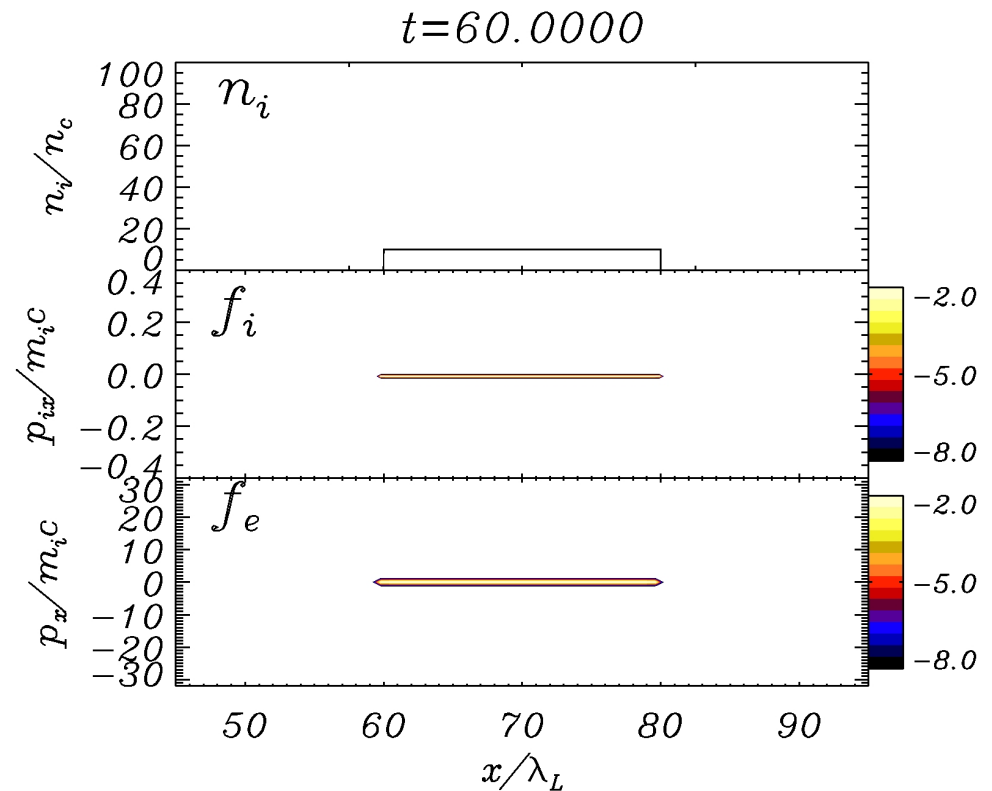
Fast ions seen in PIC simulations suggest several possible mechanisms of ion acceleration

1D PIC simulation

$$I = 3.5 \times 10^{20} \text{ W/cm}^2, \\ n_e = 10^{22} \text{ cm}^{-3}$$

Three fast ion populations, accelerated

- from **rear side** in **forward** direction
- from **front side** in **forward** direction
- from **front side** in **backward** direction



Which is the dominant “channel” for given conditions?

Fast ions seen in PIC simulations suggest several possible mechanisms of ion acceleration

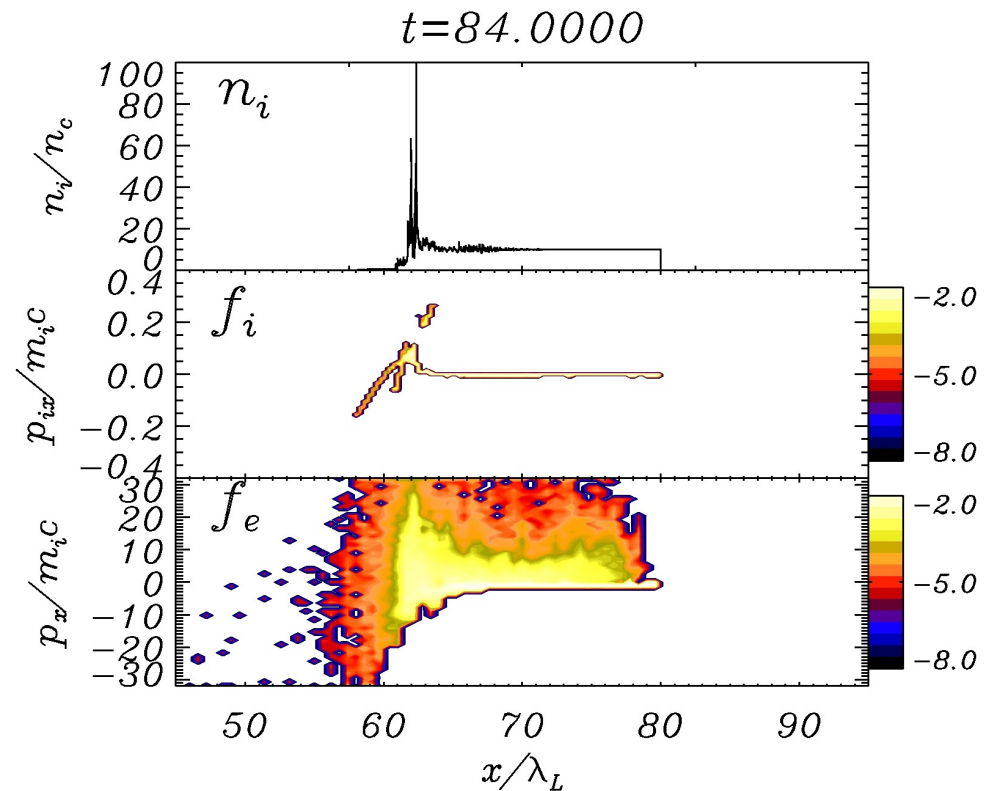
1D PIC simulation

$$I = 3.5 \times 10^{20} \text{ W/cm}^2,$$

$$n_e = 10^{22} \text{ cm}^{-3}$$

Three fast ion populations, accelerated

- from **rear side** in **forward** direction
- from **front side** in **forward** direction
- from **front side** in **backward** direction



Which is the dominant “channel” for given conditions?

Fast ions seen in PIC simulations suggest several possible mechanisms of ion acceleration

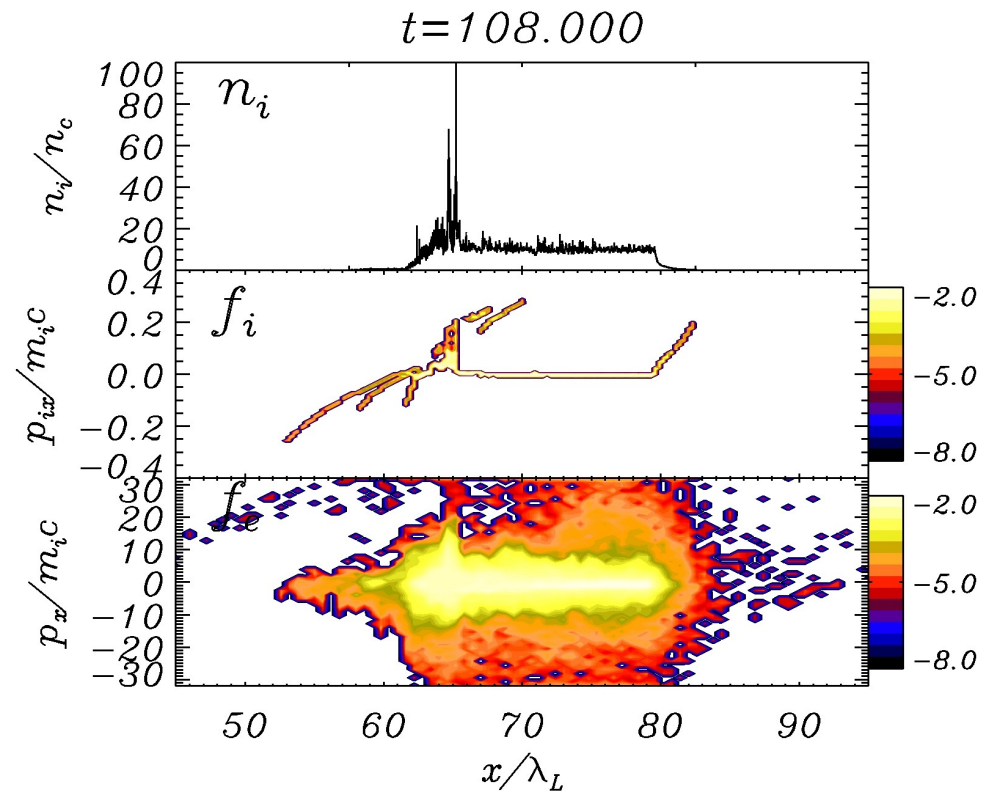
1D PIC simulation

$$I = 3.5 \times 10^{20} \text{ W/cm}^2,$$

$$n_e = 10^{22} \text{ cm}^{-3}$$

Three fast ion populations, accelerated

- from **rear side** in **forward** direction
- from **front side** in **forward** direction
- from **front side** in **backward** direction



Which is the dominant “channel” for given conditions?

Fast ions seen in PIC simulations suggest several possible mechanisms of ion acceleration

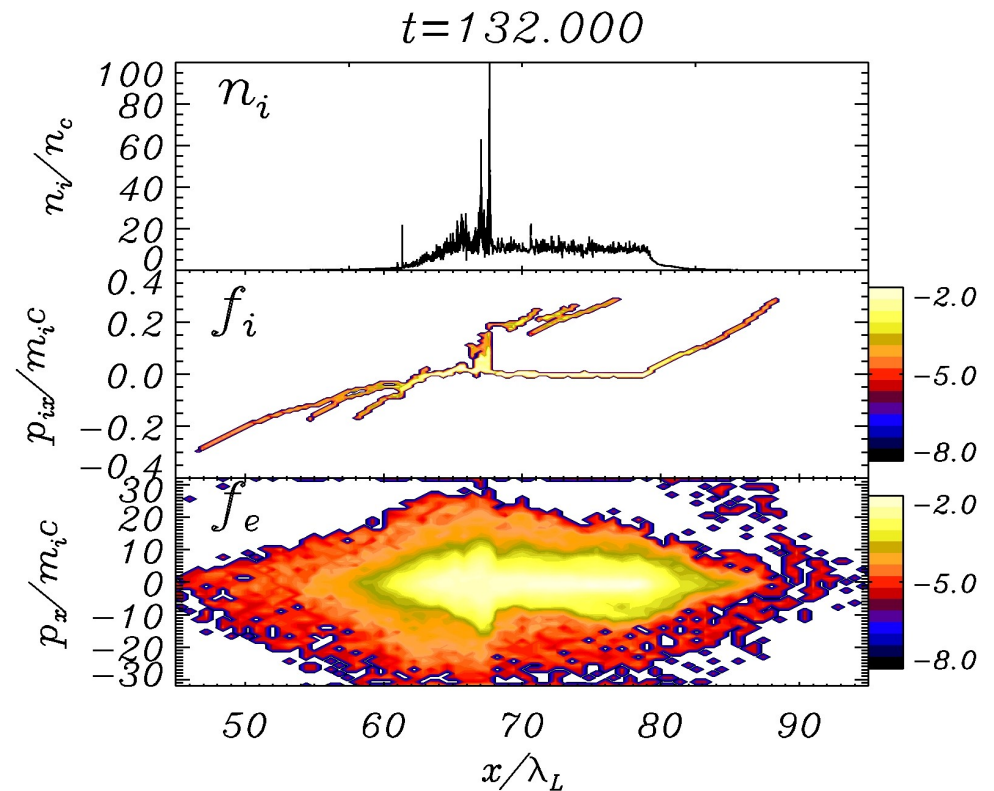
1D PIC simulation

$$I = 3.5 \times 10^{20} \text{ W/cm}^2,$$

$$n_e = 10^{22} \text{ cm}^{-3}$$

Three fast ion populations, accelerated

- from **rear side** in **forward** direction
- from **front side** in **forward** direction
- from **front side** in **backward** direction



Which is the dominant “channel” for given conditions?

Fast ions seen in PIC simulations suggest several possible mechanisms of ion acceleration

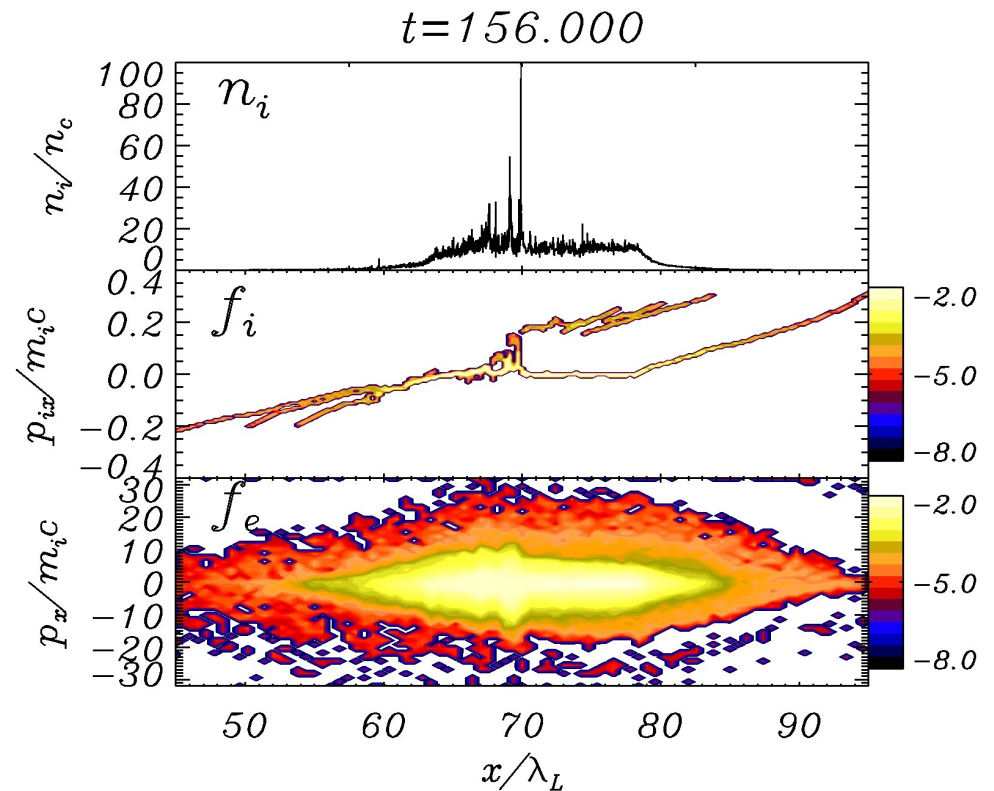
1D PIC simulation

$$I = 3.5 \times 10^{20} \text{ W/cm}^2,$$

$$n_e = 10^{22} \text{ cm}^{-3}$$

Three fast ion populations, accelerated

- from **rear side** in **forward** direction
- from **front side** in **forward** direction
- from **front side** in **backward** direction



Which is the dominant “channel” for given conditions?

The “front vs rear side” debate

Clark et al: “It is likely that the protons originate from the front surface of the target and are bent by large magnetic fields which exist in the target interior.”

Maksimchuk et al: “The protons [...] appear to originate from impurities on the front side of the target [...] The maximum proton energy can be explained by the charge-separation electrostatic-field acceleration due to vacuum heating.

Snavely et al: “We have concluded that light pressure effects at the front surface focal spot on the target could not generate the observed ions because of the clear evidence that the protons are emitted perpendicular to the rear surface(s) of the target.”

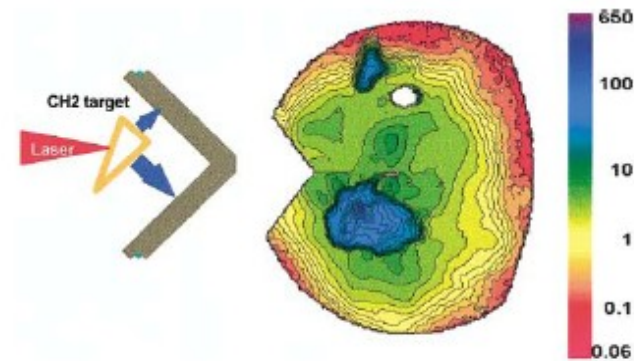
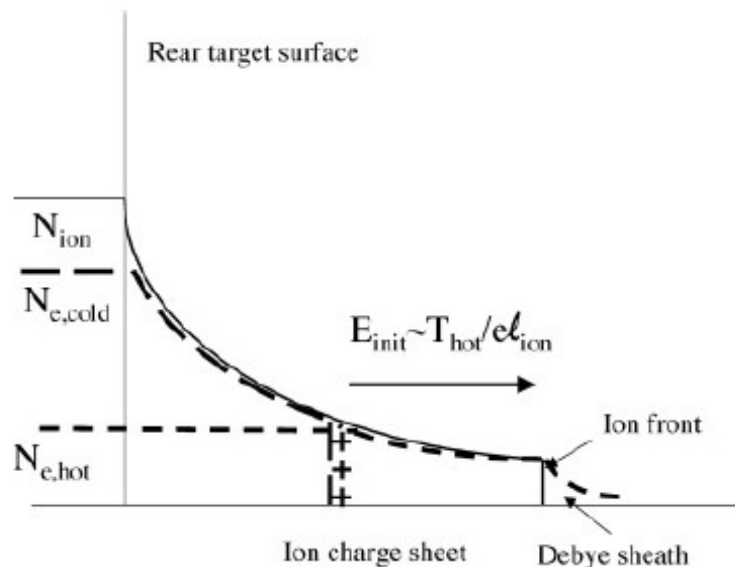
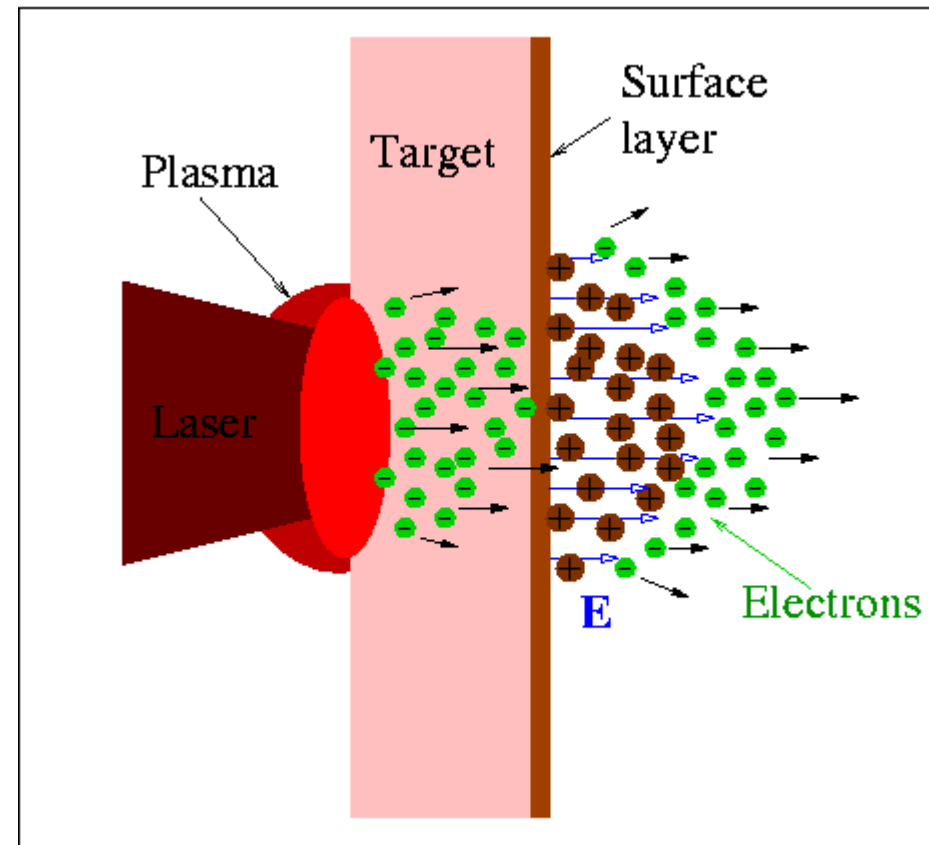


FIG. 4 (color). Contours of dose in krad as a function of angle recorded on a RC film through $300 \mu\text{m Ta}$ (proton $E > 18 \text{ MeV}$). The image clearly shows two proton beams, the larger from the major face and the smaller from the minor face of the wedge.

The Target Normal Sheath Acceleration model of proton acceleration

Physical mechanism:
acceleration in the space-charge
electric field generated by
“fast” electrons
escaping from the target



[S. Wilks et al, Phys. Plasmas **8** (2001) 542]

Modeling of sheath acceleration: the problem of plasma expansion in vacuum

Analytical approach:

- electrostatic approximation
- fluid ions
- electrons in Boltzmann equilibrium
- “fast” electron temperature and density as input parameters

“Mora's formula” from isothermal, semi-infinite slab model

[P.Mora, PRL **90** (2003) 185002]

- diverges with time (infinite energy available!)
- “corrected” assuming finite acceleration time t_p

$$n_e = n_0 \exp\left(\frac{e\Phi}{k_B T_e}\right), \quad \nabla^2 \Phi = Z e n_i - e n_e$$

$$M_i \frac{d\mathbf{v}_i}{dt} = Ze\mathbf{E} = -Ze\nabla\Phi, \quad \partial_t n_i = \nabla \cdot (n_i \mathbf{v}_i)$$

$$v_i \simeq 2c_s \ln\left(\omega_{pi} t_p + \sqrt{\omega_{pi}^2 t_p^2 + 1}\right)$$

$$c_s = \sqrt{Z k_B T_e / m_i}$$

[J.Fuchs et al, Nature Phys. **2** (2005) 48]

Modeling of sheath acceleration: the problem of plasma expansion in vacuum

Analytical approach:

- electrostatic approximation
- fluid ions
- electrons in Boltzmann equilibrium
- “fast” electron temperature and density as input parameters
- **thin slab** to account for **finite energy**

Comparison with numerical PIC results (including kinetic effects):

$$n_e = n_0 \exp\left(\frac{e\Phi}{k_B T_e}\right), \quad \nabla^2 \Phi = Z e n_i - e n_e$$

$$M_i \frac{d\mathbf{v}_i}{dt} = Z e \mathbf{E} = -Z e \nabla \Phi, \quad \partial_t n_i = \nabla \cdot (n_i \mathbf{v}_i)$$

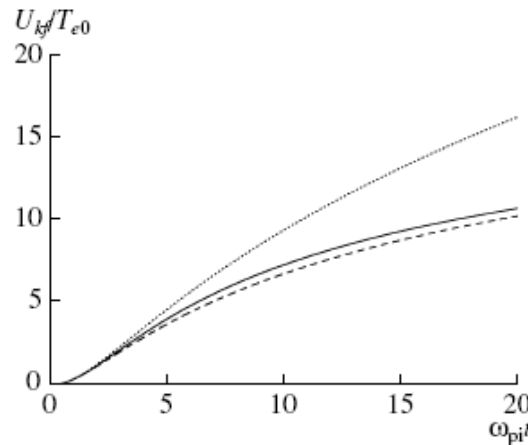


Fig. 3. The kinetic energy acquired by the fastest ion during the expansion of a slab of total thickness $2a = 40$ as predicted by the numerical simulations (solid line), by the analytical model (dashed line), and by the semi-infinite model [11] (dotted line).

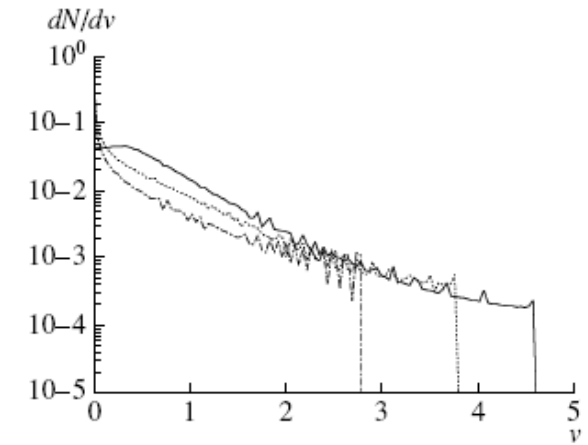


Fig. 4. Ion velocity spectrum at $\tau = 5$ (dashed line), $\tau = 10$ (dotted line), and $\tau = 20$ (solid line). The initial slab total size is $2a = 40$ and v is normalized to the initial sound speed.

How to diagnose the electric fields directly?

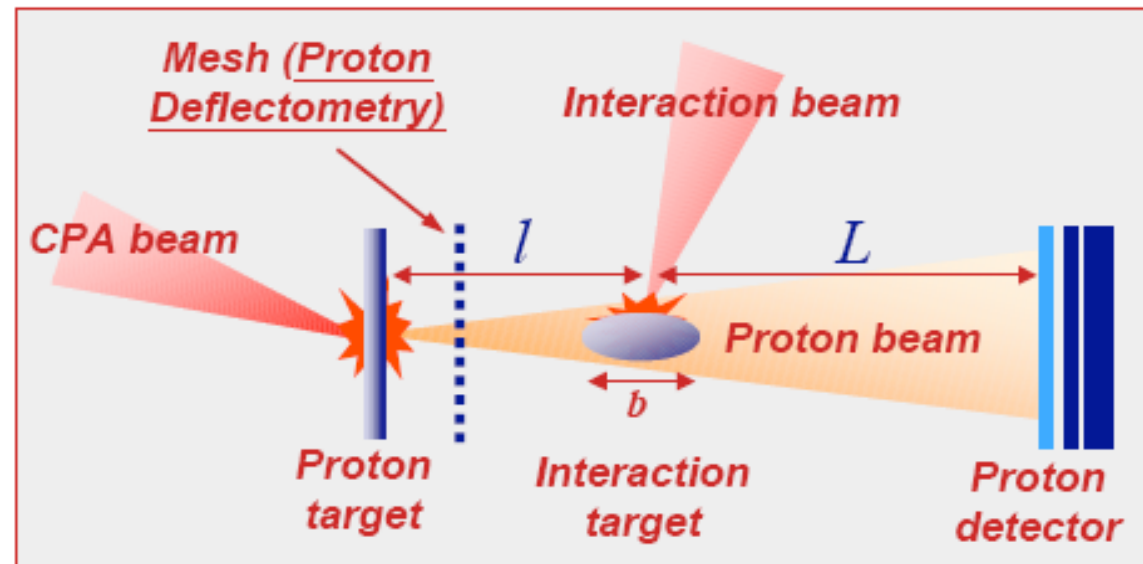
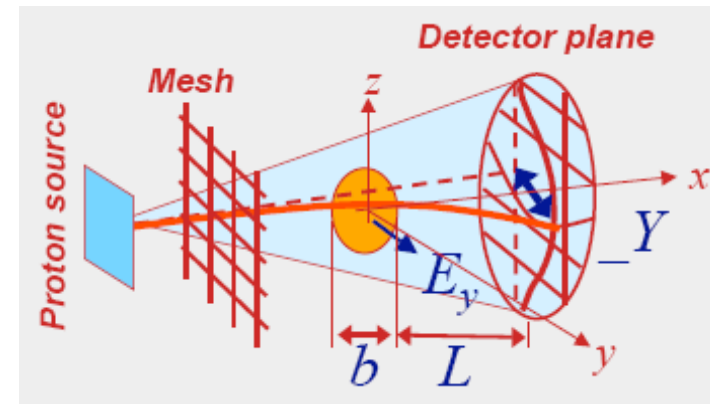
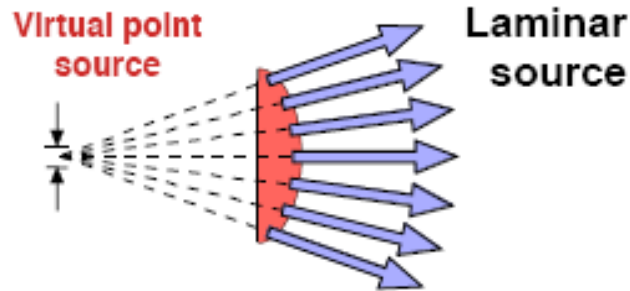
Idea: use the protons as a probe

Due to high laminarity the proton beam has **imaging properties**

The short duration of the proton burst allows **picosecond temporal resolution**

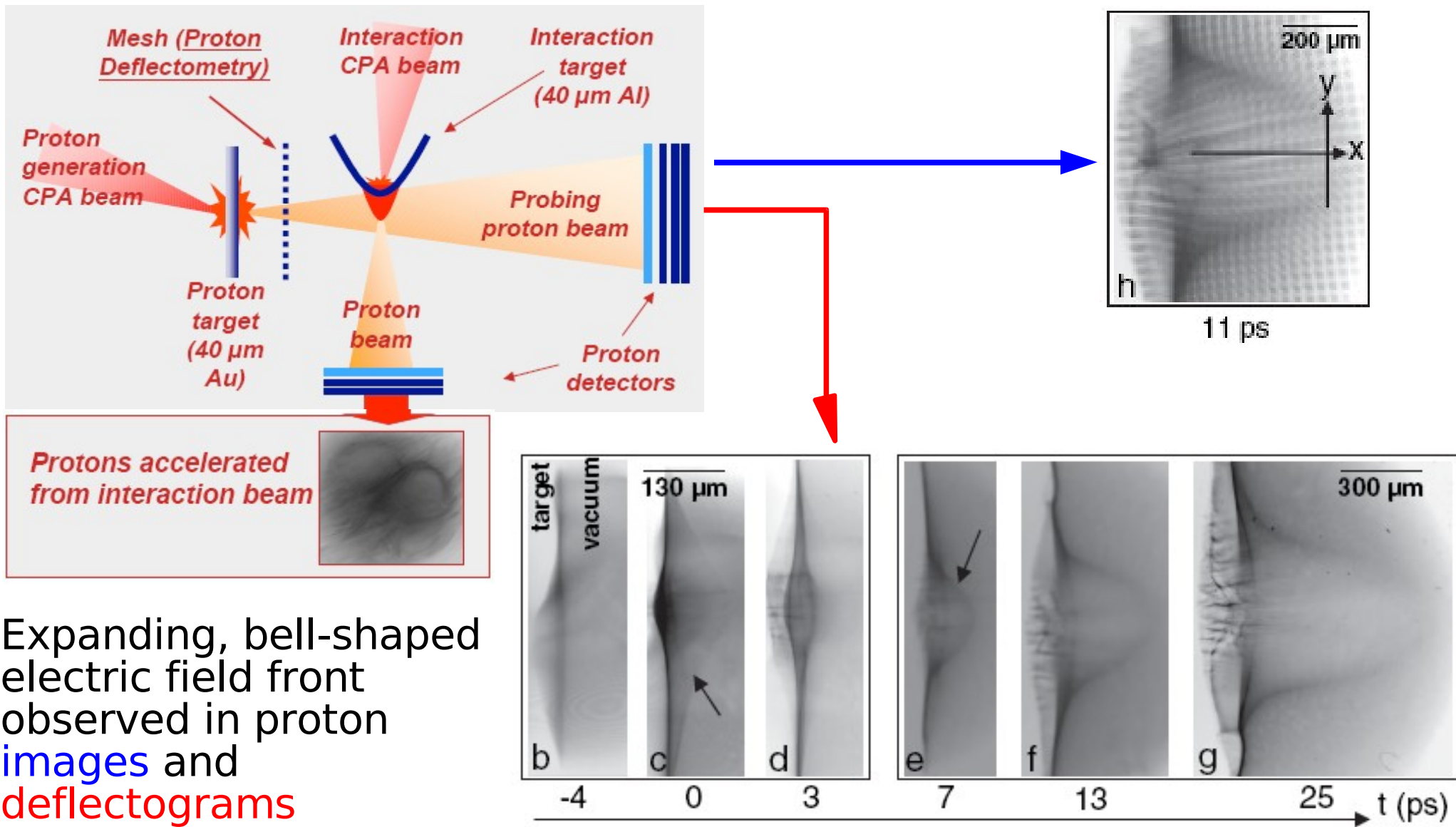
Protons of a given energy will cross the probed object at a particular time. An energy-resolving detector (e.g. Radiochromic Film) thus provides **multiframe capability**

In a laser-plasma experiment the proton probe is easily **synchronized with the interaction**



Borghesi et al, Phys.Plasmas **9** (2002) 2214
Borghesi et al, Phys.Rev.Lett. **92** (2004) 055003
Cowan et al, Phys.Rev.Lett. **92** (2004) 204851

Experimental detection of sheath fields using the proton diagnostic

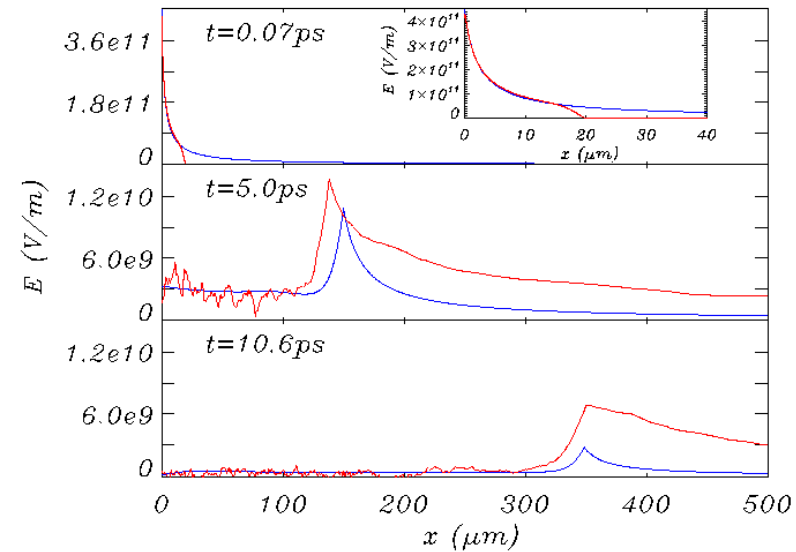
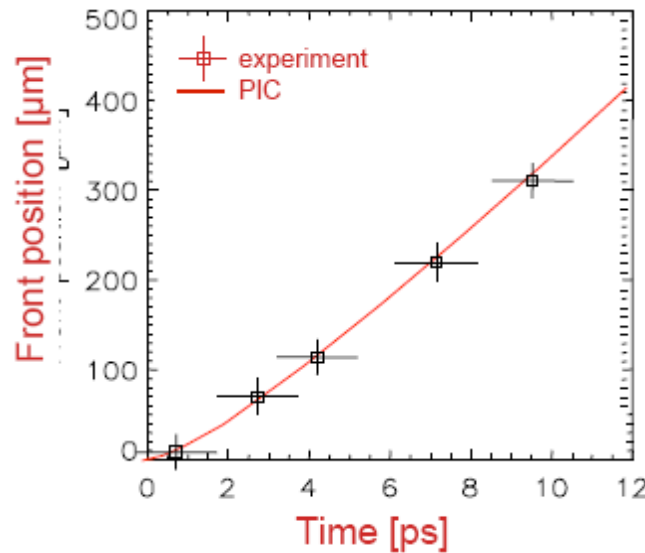


Expanding, bell-shaped electric field front observed in proton images and deflectograms

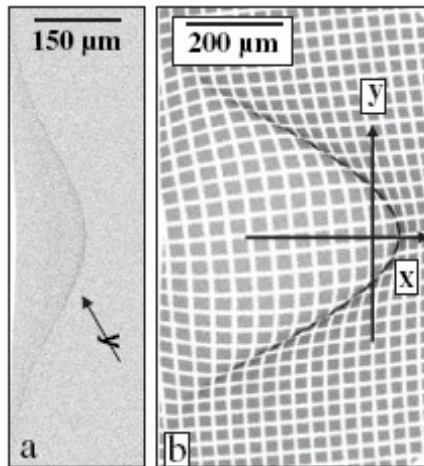
L. Romagnani, J. Fuchs, M. Borghesi, P. Antici, P. Audebert, F. Ceccherini, T. Cowan, T. Grismayer, S. Kar, A. Macchi, P. Mora, G. Pretzler, A. Schiavi, T. Toncian, O. Willi, Phys. Rev. Lett. **95** (2005) 195001

Experimental detection of sheath fields using the proton diagnostic

Experimental results have been compared with **PIC simulations** using the plasma expansion model.

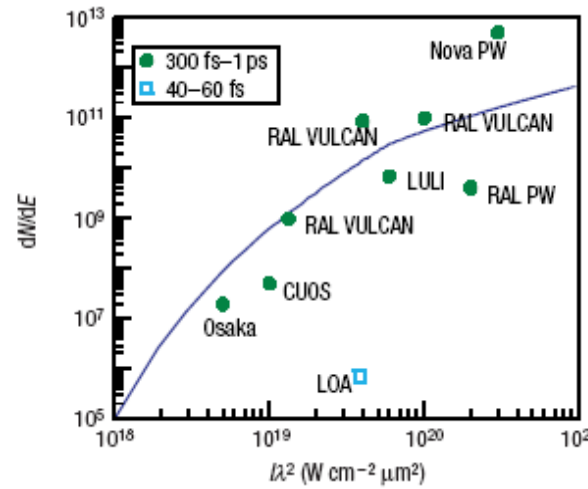
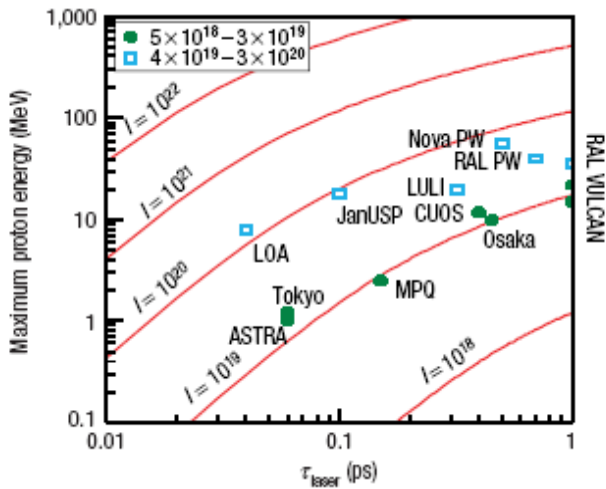


Particle tracing simulations of proton deflection in the **PIC fields** (plus an “heuristic” modeling of the 2D expansion) fit well experimental images and deflectograms



Comparison of **fluid** and **kinetic (PIC)** results show the importance of kinetic and non-thermal effects in the plasma expansion

Experimental State of the Art (quick look)



Scaling of **ion energy** and **number** vs. pulse duration and irradiance checked vs. "modified" Mora's isothermal model

From: M. Borghesi et al, Fusion Science & Technology **49** (2006) 412;
J. Fuchs et al, Nature Physics **2** (2005) 48 .

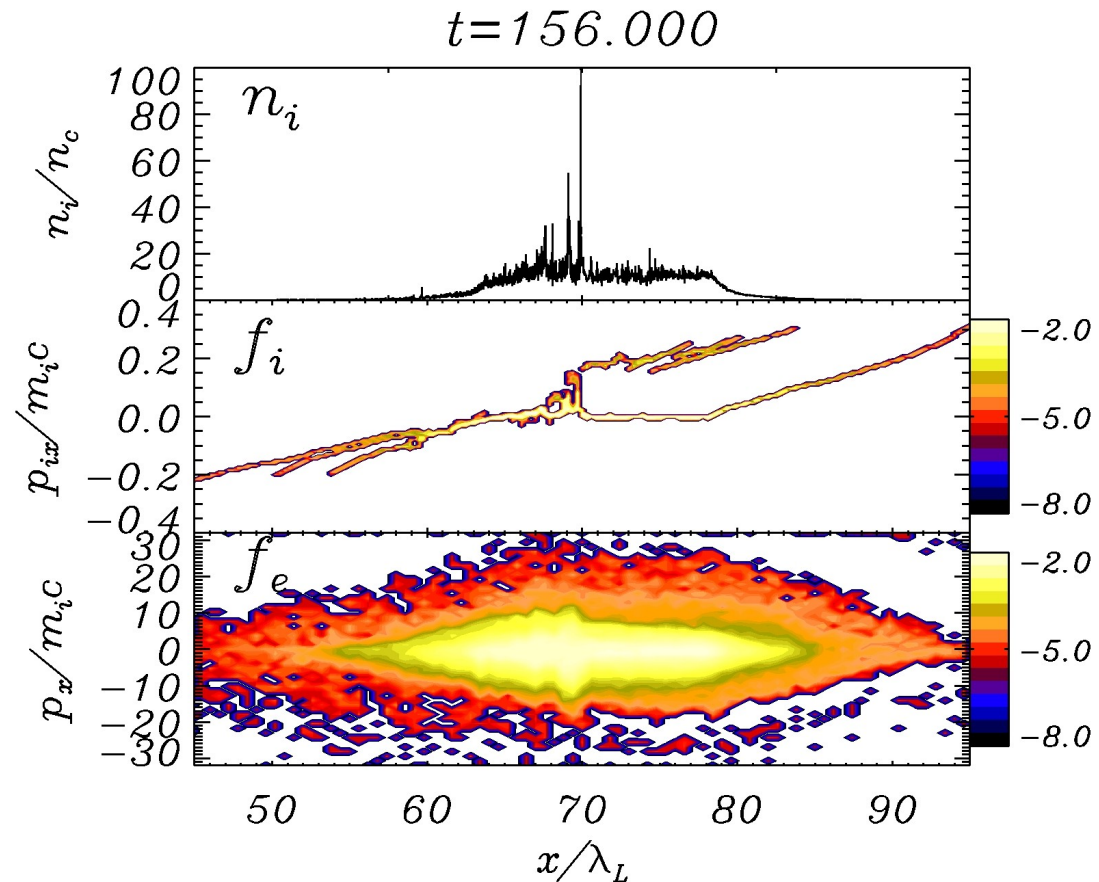
A few recent results, all based on TNSA:

- **narrow energy spectrum of protons from engineered double-layer target** [H. Schwoerer et al, Nature **439** (2006) 445]
- **MeV carbon ions from pre-heated ("decontaminated") target** [B. Hegelich et al, Nature **439** (2006) 441]
- **Ultrafast "laser-plasma microlens" for ion beam focusing and energy selection** [T. Toncian et al, Science **312** (2006) 410]

What about other ion populations?

For prepulse-free measurement, the density profile is sharp also at the front side: TNSA in backward direction observed for thin targets (electrons have time to reflux back)

T.Ceccotti et al, PRL **99** (2007) 185002

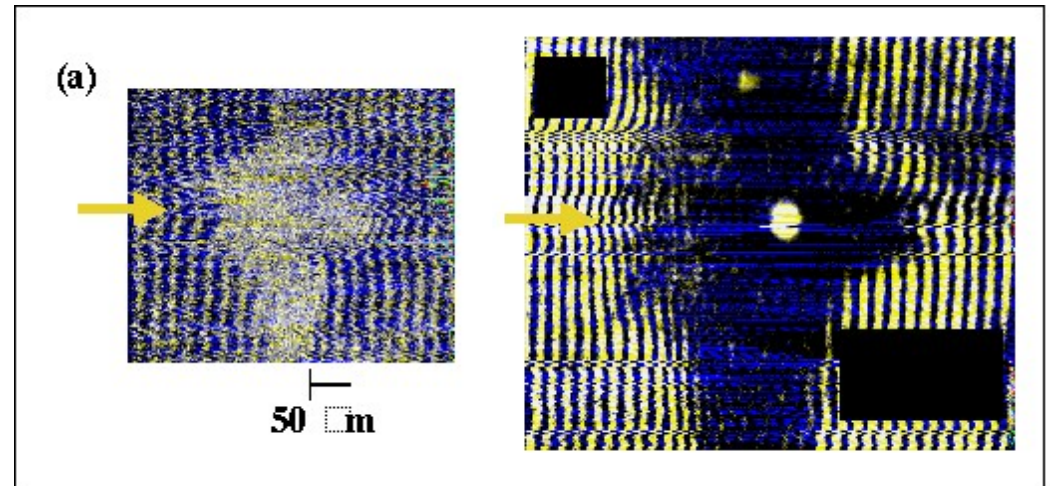


What about other ion populations?

For prepulse-free measurement, the density profile is sharp also at the front side: TNSA in backward direction observed for thin targets (electrons have time to reflux back)

T.Ceccotti et al, PRL **99** (2007) 185002

In petawatt ($I \sim 10^{20} \text{ W/cm}^2$) experiments for “quite thin” targets a highly collimated dense plasma jet from the rear side is observed: due to front side ions?



(absence of jet for larger thickness ascribed to collisional ion stopping in the target)

S.Kar, M.Borghesi, S. V. Bulanov, A.J.MacKinnon, P.K.Patel, M.Key, L.Romagnani, A.Schiavi, A.Macchi, O.Willi, RAL CLF annual report 2003-2004, p.24, submitted to PRL

Simulations suggest regime transition at intensities $\sim 10^{21}$ W/cm²

Results from “multi-parametric” PIC simulations:

- for maximal ion energy an optimal areal density $n_e d$ exists for given intensity I

- ion energy scales with laser energy \mathcal{E}_L

as $\mathcal{E}_L^{1/2}$ for $I < 10^{21}$ W/cm²

as \mathcal{E}_L for $I > 10^{21}$ W/cm²

- transition is explained by the dominance of **Radiation Pressure Acceleration**

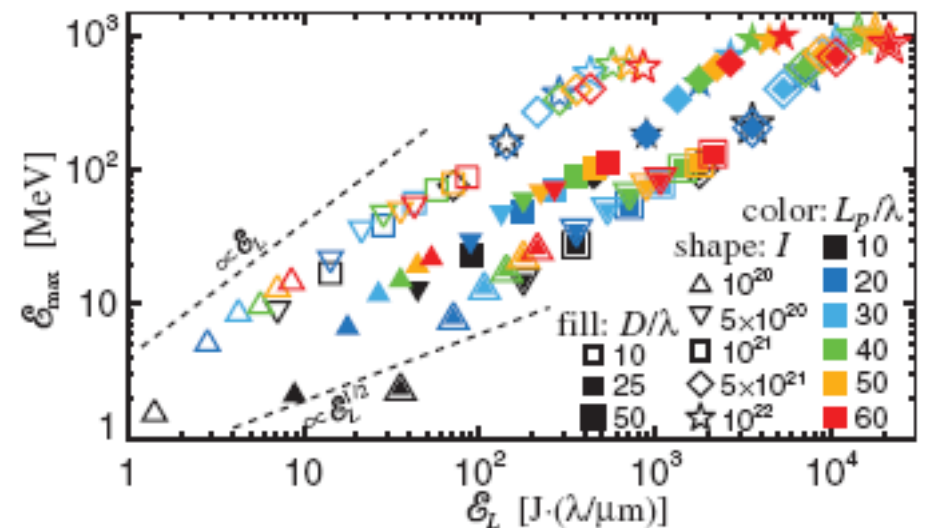


FIG. 3 (color). Proton maximum energy vs laser pulse energy for $l = \lambda$, $n_e = 100n_{\text{cr}}$. The dashed lines exemplify possible scalings.

Relativistic ions: the “*Laser-Piston*” regime

Ultra-relativistic interaction regime
 “dominated by radiation pressure”

T.Esirkepov, M.Borghesi, S.V.Bulanov,
 G.Mourou, T.Tajima, PRL **92**, 175003 (2004)

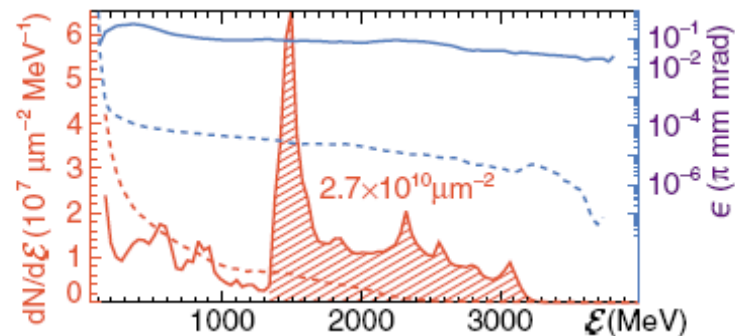
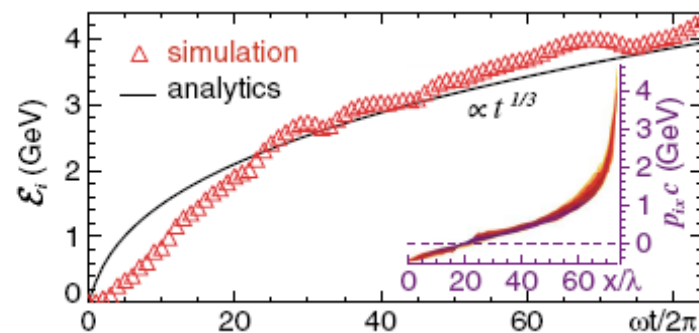
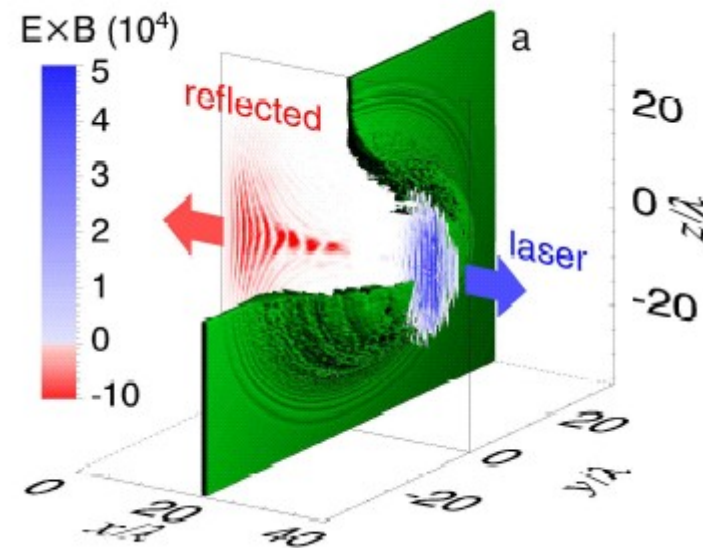
Required laser intensity

$$I \geq 10^{23} \text{ W/cm}^2$$

The foreseen ion beam parameters
 make this attractive as a driver of
 low-energy neutrino sources
 for studies of CP violation

in $\nu_{\mu} \rightarrow \nu_e$ oscillations

S.V.Bulanov, T.Esirkepov, P.Migliozzi, F.Pegoraro,
 T.Tajima, F.Terranova, NIM A **540**, 133 (2005);
 F. Terranova, S.V.Bulanov, J.L.Collier, H.Kiriyama,
 F.Pegoraro, NIM A **558**, 430 (2006).



Old motivations for Radiation Pressure Acceleration

22

NATURE

JULY 2, 1966 VOL. 211

INTERSTELLAR VEHICLE PROPELLED BY TERRESTRIAL LASER BEAM

By PROF. G. MARX

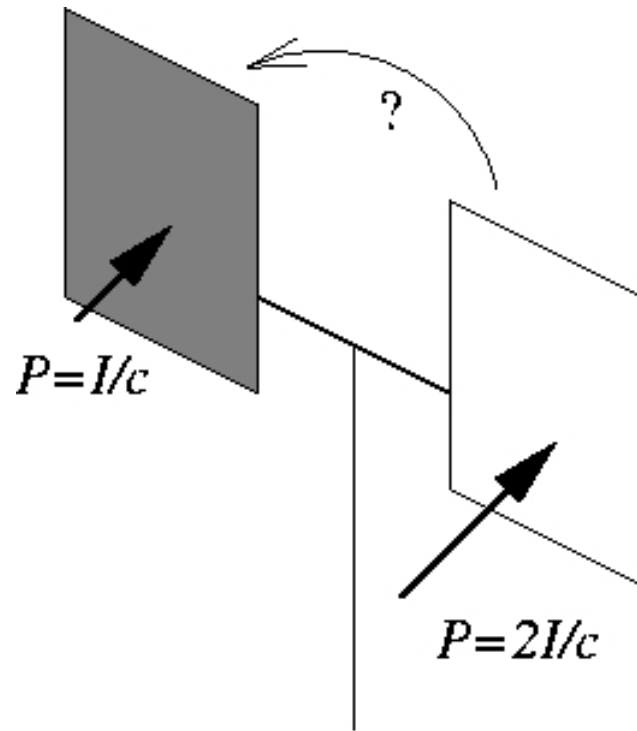
Institute of Theoretical Physics, Roland Eötvös University, Budapest

Analysis based on relativity and a **rigid mirror** acceleration model suggests **100% efficiency** as $V \rightarrow c$

$$\beta = \frac{v_i}{c} = \frac{(1 + 2\tau)^2 - 1}{(1 + 2\tau)^2 + 1}$$

$$\eta = \frac{2\tau}{2\tau + 1}, \quad \tau = \frac{ISt}{Mc^2}$$

Maximize the effect of Radiation Pressure: the “optical mill” (Solar radiometer) example

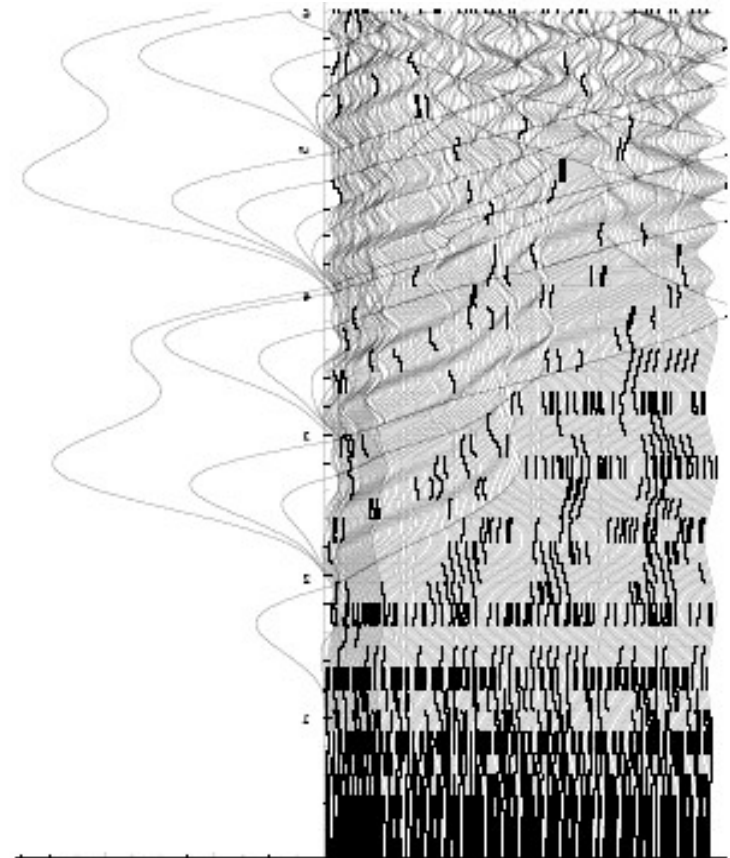
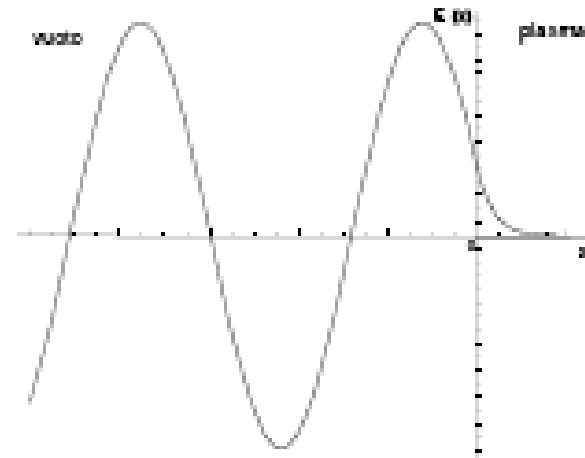
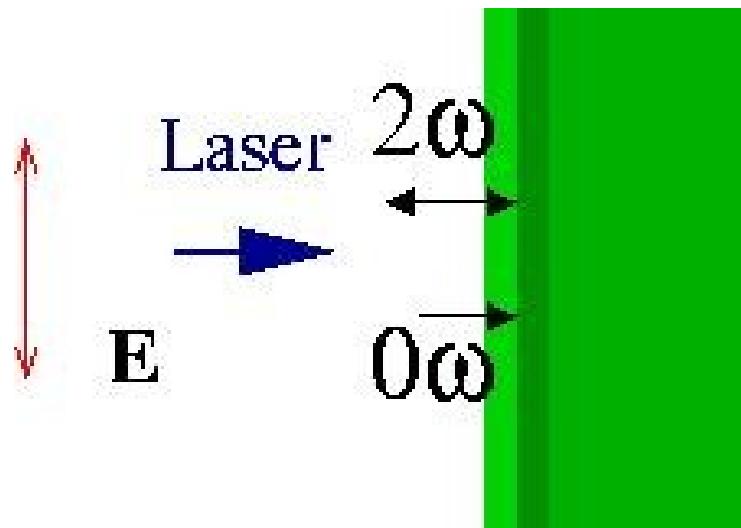


The mill spins in the **opposite** direction to what we'd expect thinking of P_{rad} only: the heating of the **black** (absorbing) surface increased the **thermal pressure** of the background gas (imperfect vacuum!)

In the high-intensity irradiation of a solid-density (plasma) target, “heating” is due to energy absorption into **electrons**

How to “switch off” fast electrons

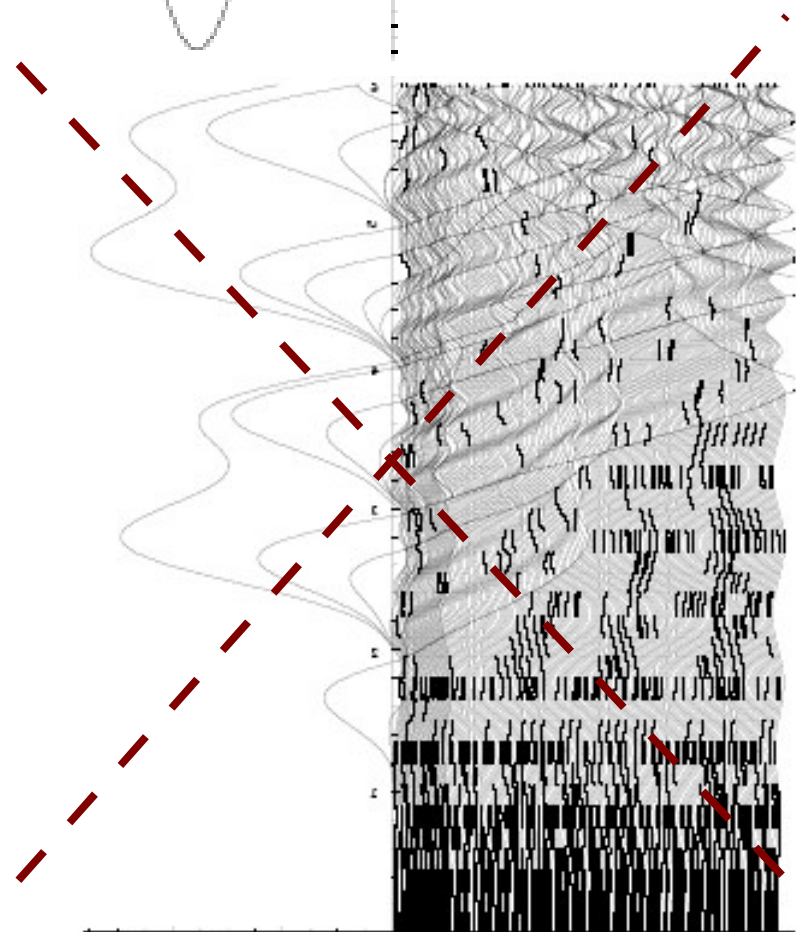
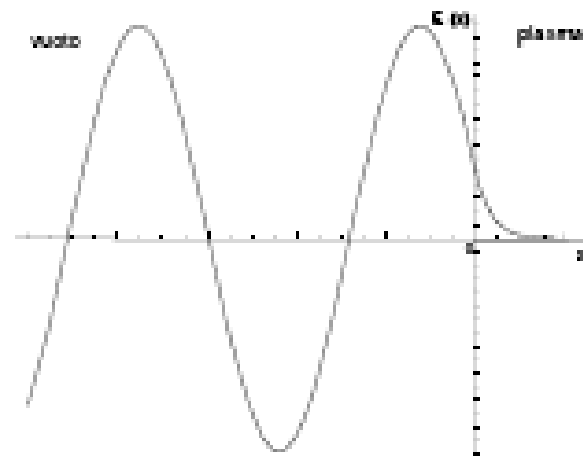
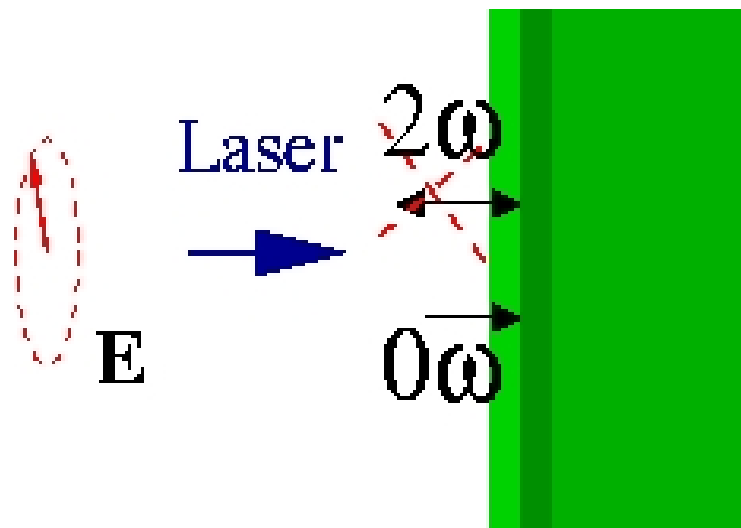
Forced oscillations of the electrons across the plasma-vacuum interface ($L \ll \lambda$) driven by the 2ω component of the $\mathbf{J} \times \mathbf{B}$ force (normal incidence) are non-adiabatic and lead to electron acceleration



How to “switch off” fast electrons

- For **circular polarization**,
the 2ω component of the $\mathbf{J} \times \mathbf{B}$
force vanishes:
- **inhibition** of electron acceleration
 - **“direct” ion acceleration**

(i.e. “**dominance**” of
Radiation Pressure)



A.Macchi, F.Cattani, T.V.Liseikina, F. Cornolti,
Phys.Rev.Lett **94**, 165003 (2005)

S. Tuveri, tesi di Laurea, 2006

Features of Ion Acceleration with Circular Polarization

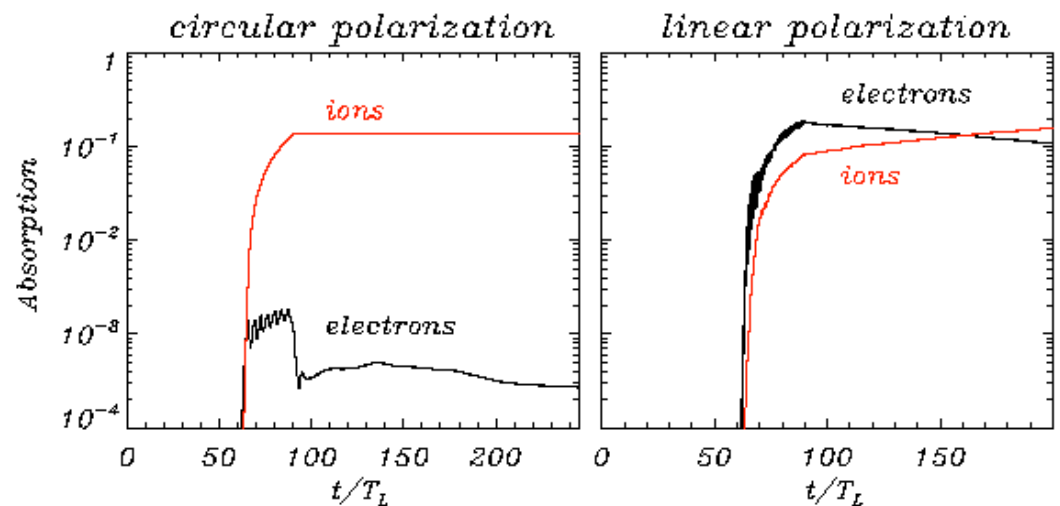
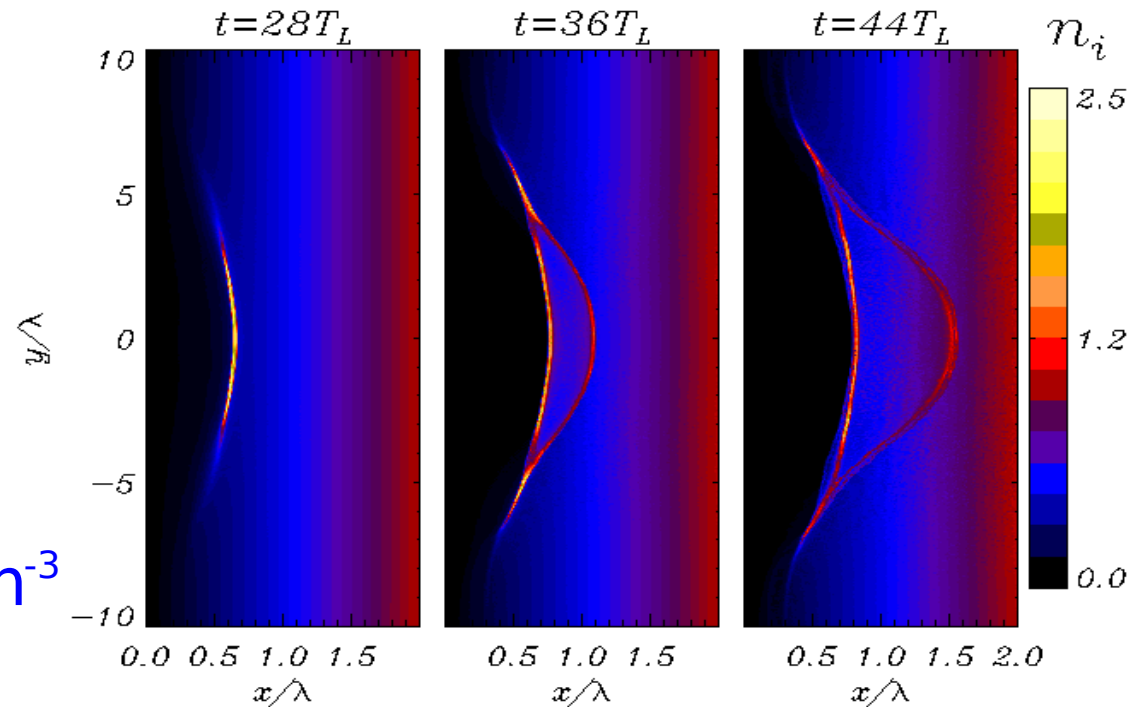
[Macchi et al, PRL **94** (2005) 165003;
Liseikina and Macchi, APL **91** (2007) 171502]

1D and 2D PIC simulations,
“thick” targets
 $I=10^{18}-10^{21}$ W/cm² ,
 $\tau=10-100$ fs

Features at
 $I=3.5 \times 10^{20}$ W/cm² , $n_e=10^{22}$ cm⁻³

- efficiency = 14%
- angular spread < 5 deg.
- mean energy = 10 MeV
- energy spread 20%

production of a
single ultrashort ion bunch
possible with shorter pulses



Features of Ion Acceleration with Circular Polarization

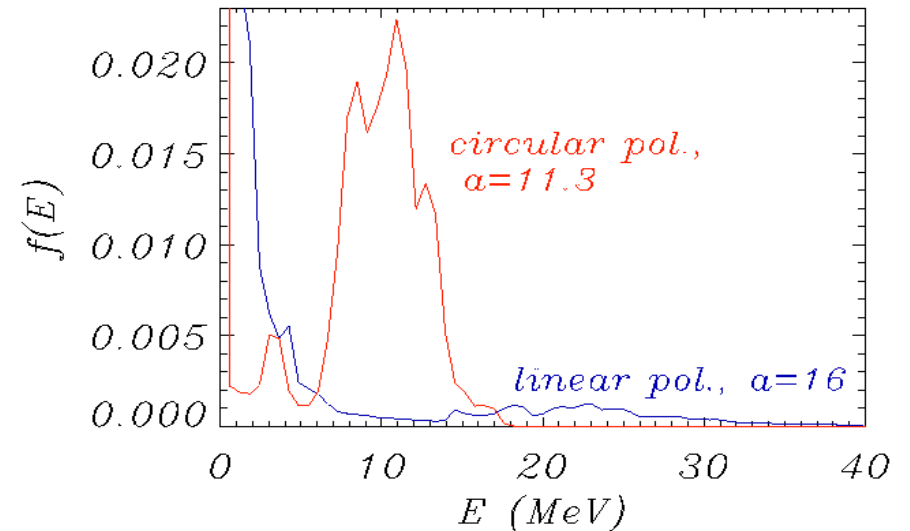
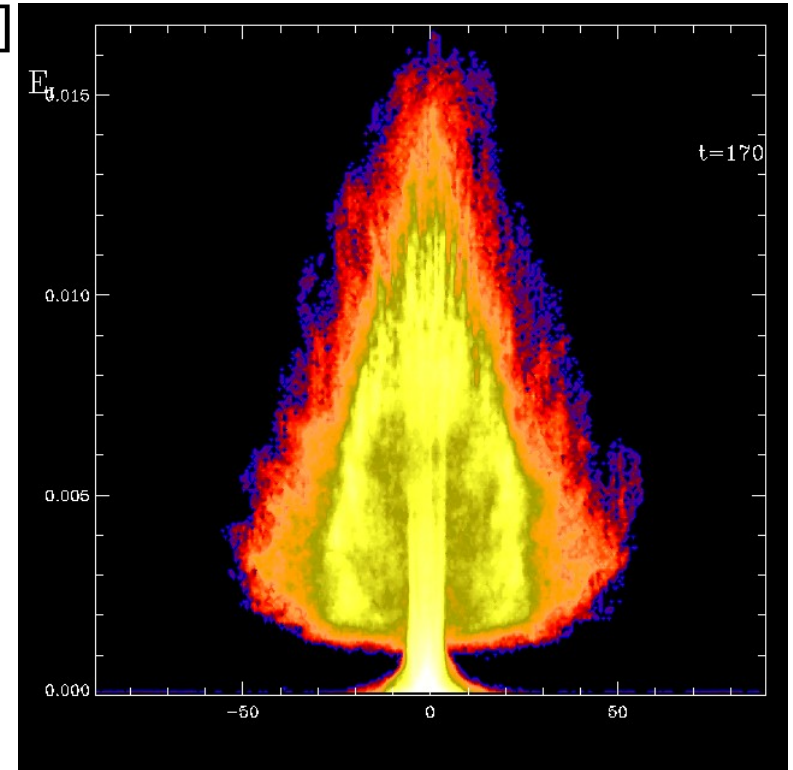
[Macchi et al, PRL **94** (2005) 165003;
Liseikina and Macchi, APL **91** (2007) 171502]

1D and 2D PIC simulations,
“thick” targets
 $I=10^{18}-10^{21}$ W/cm² ,
 $\tau=10-100$ fs

Features at
 $I=3.5 \times 10^{20}$ W/cm² , $n_e=10^{22}$ cm⁻³

- efficiency = 14%
- angular spread < 5 deg.
- mean energy = 10 MeV
- energy spread 20%

production of a
single ultrashort ion bunch
possible with shorter pulses



Features of Ion Acceleration with Circular Polarization

[Macchi et al, PRL **94** (2005) 165003;
Liseikina and Macchi, APL **91** (2007) 171502]

1D and 2D PIC simulations,
“thick” targets

$l=1$

$\tau=1$

Feat

$l=3$

•effic

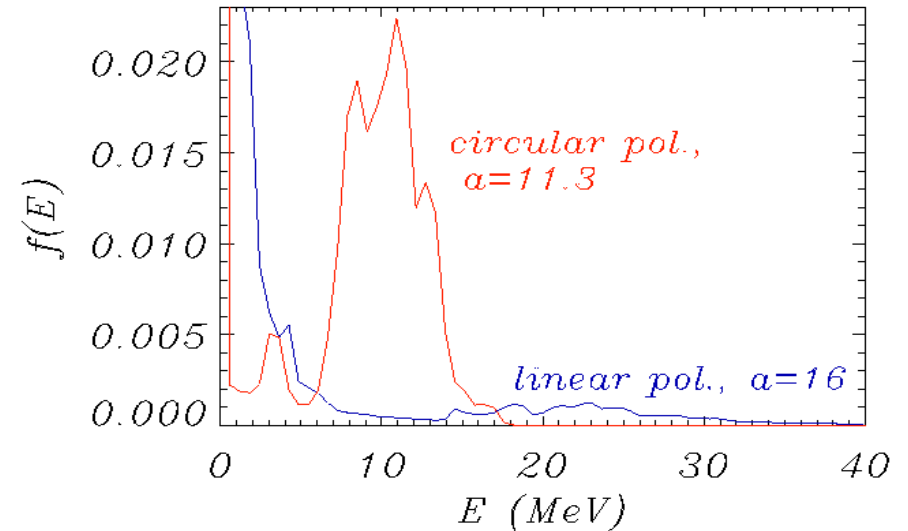
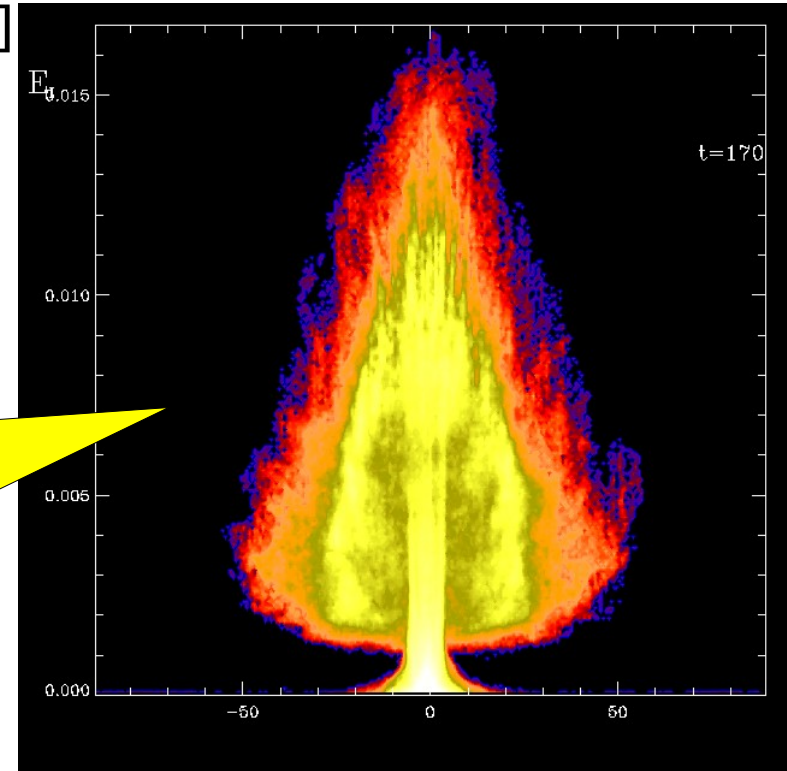
•ang

•mea

•ene

production of a
single ultrashort ion bunch
possible with shorter pulses

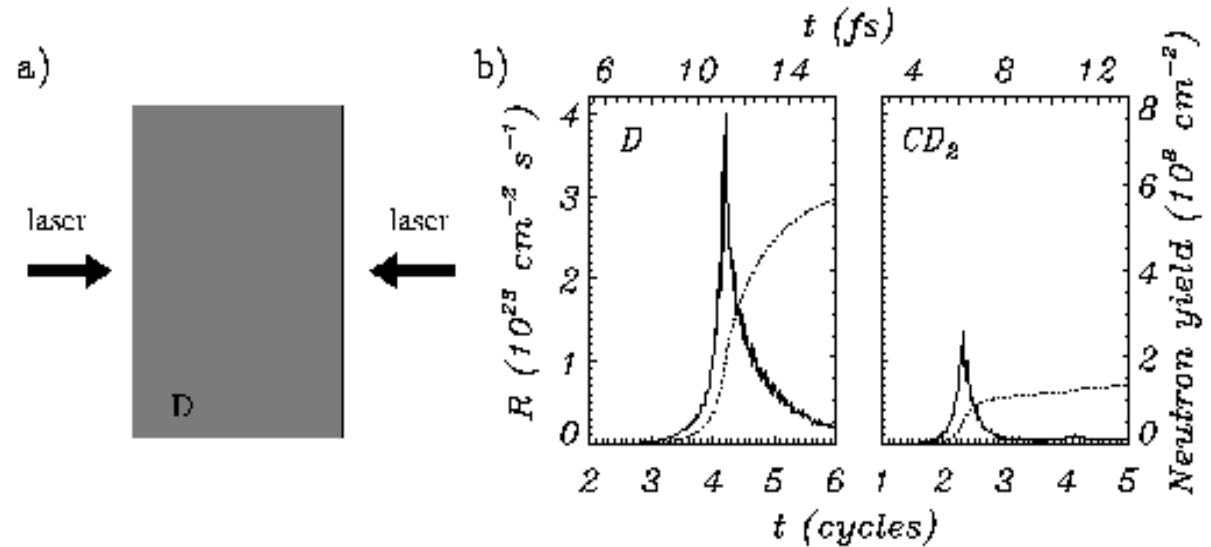
The “Xmas tree” is a contour plot of ion energy vs. emission angle, showing a high and energy-dependent collimation (submitted to *IEEE - Images in Plasma Science*)



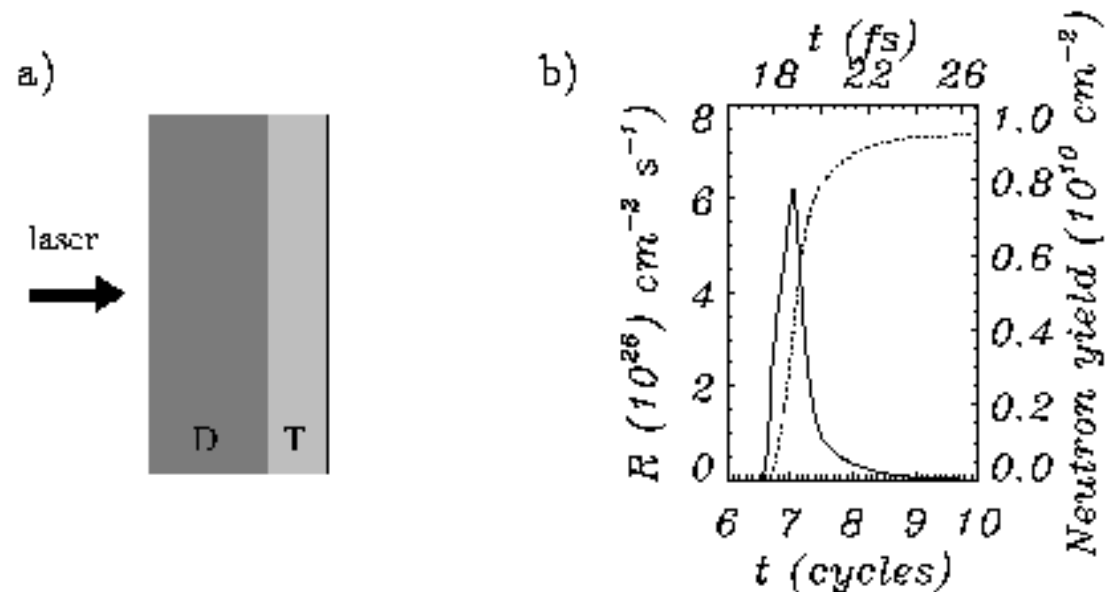
An application of circularly polarized LIA

Driver of **beam fusion** reactions in D or DT targets for a proposed scheme of a **femtosecond source of MeV neutrons**

[A. Macchi, Appl.Phys.B **82**, 337 (2006)]



A source for ultrafast control of nuclear processes and time-resolved spectroscopy of nuclei?



RPA of a thin foil

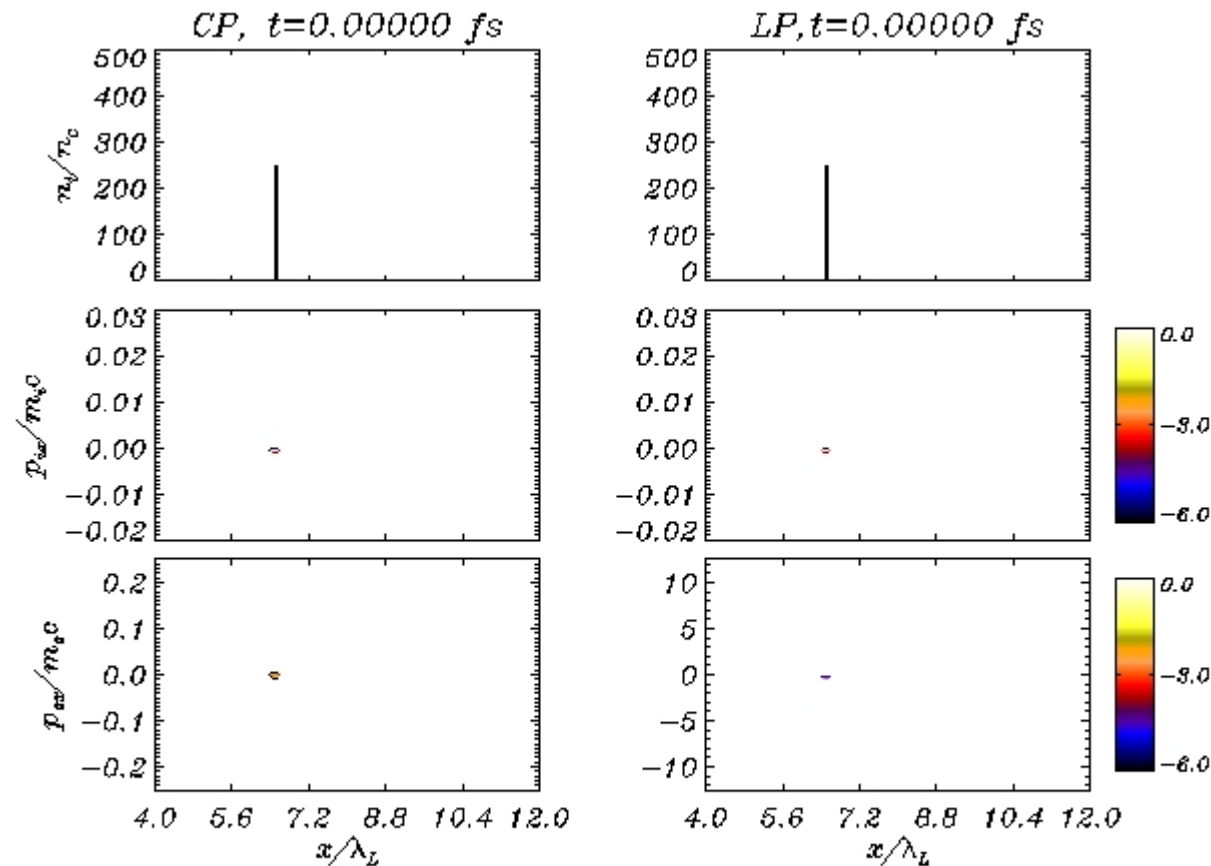
- For target thickness $d < v_i t_p$ “repeated” or “multi-staged” RPA of all the target ions occurs.
- **Circular polarization** plus **ultrathin targets** (plus **ultrahigh contrast?**) is promising for high energy (**GeV**) with intensities $\sim 10^{21}$ W/cm²

[X.Zhang et al, Phys. Plasmas **14** (2007) 073101;
A.P.L.Robinson et al, arXiv:0708.2040;
O. Klimo et al, submitted to Phys. Rev. E]

- In this regime the ion energy scales with pulse duration t_p at given intensity

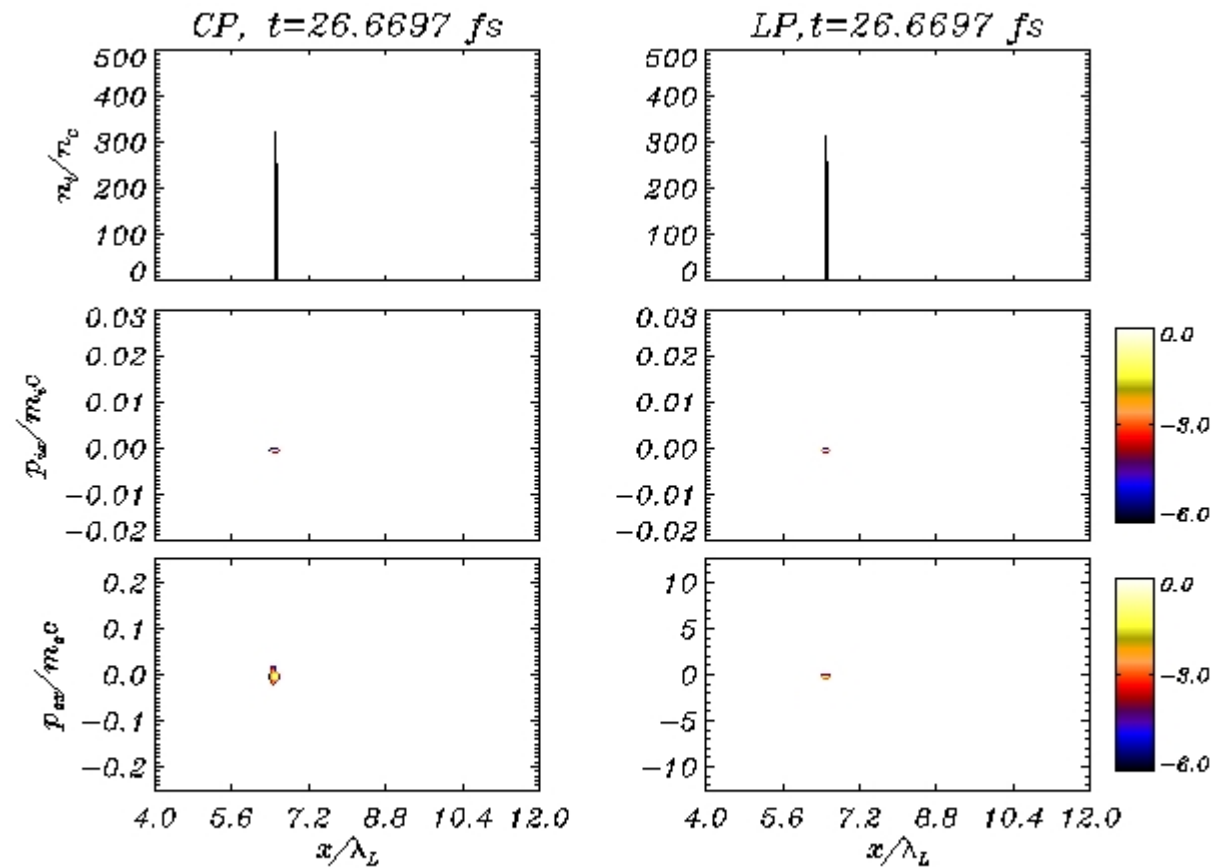
Simulation of thin foil RPA with FLAME parameters

- Carbon target, thickness $d=0.04\mu\text{m}$, $n_e = 250n_c = 4.3 \times 10^{23} \text{ cm}^{-3}$
- Laser: 26 fs pulse, average intensity $I=1.8 \times 10^{20} \text{ W/cm}^2$
relativistic peak amplitude $a_0 = 13$
- comparison of Linear Polarization vs Circular Polarization case



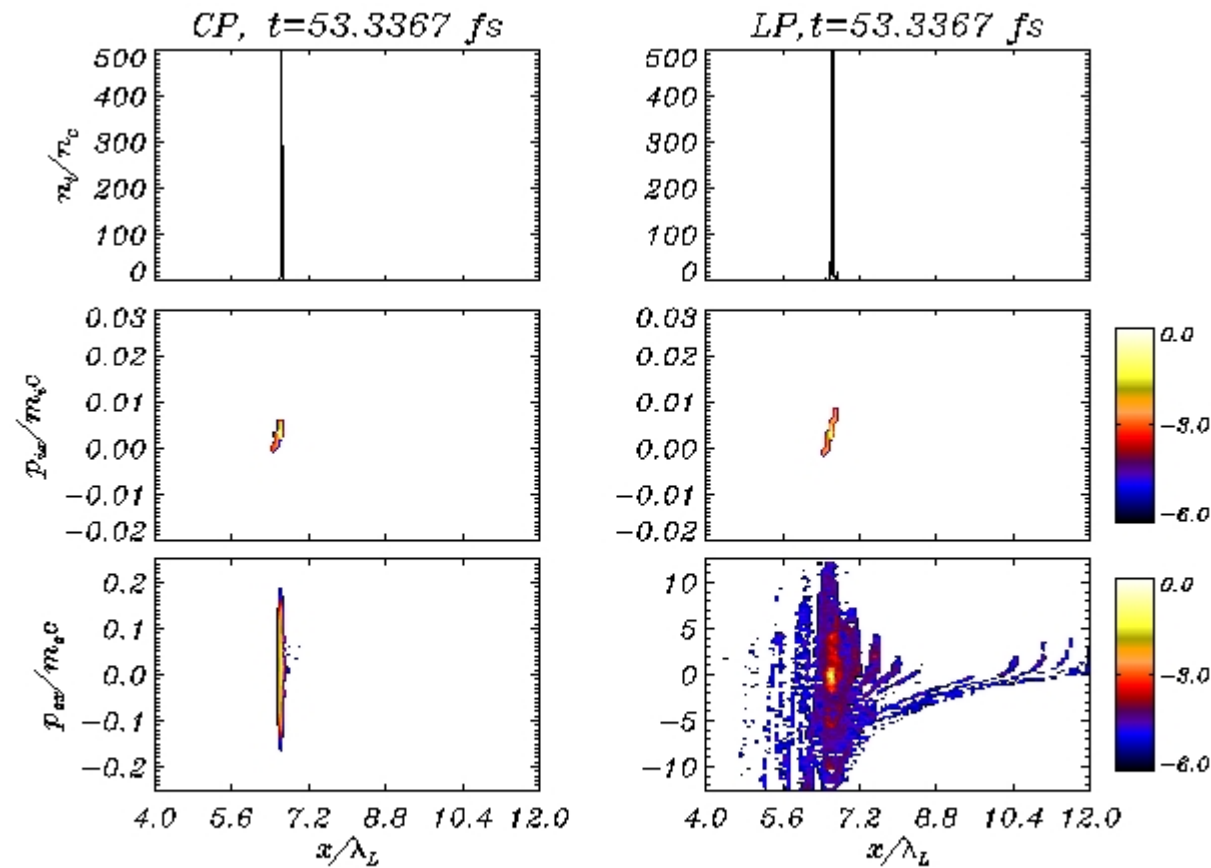
Simulation of thin foil RPA with FLAME parameters

- Carbon target, thickness $d=0.04\mu\text{m}$, $n_e = 250n_c = 4.3 \times 10^{23} \text{ cm}^{-3}$
- Laser: 26 fs pulse, average intensity $I=1.8 \times 10^{20} \text{ W/cm}^2$
relativistic amplitude $a_0 = 13$
- comparison of Linear Polarization vs Circular Polarization case



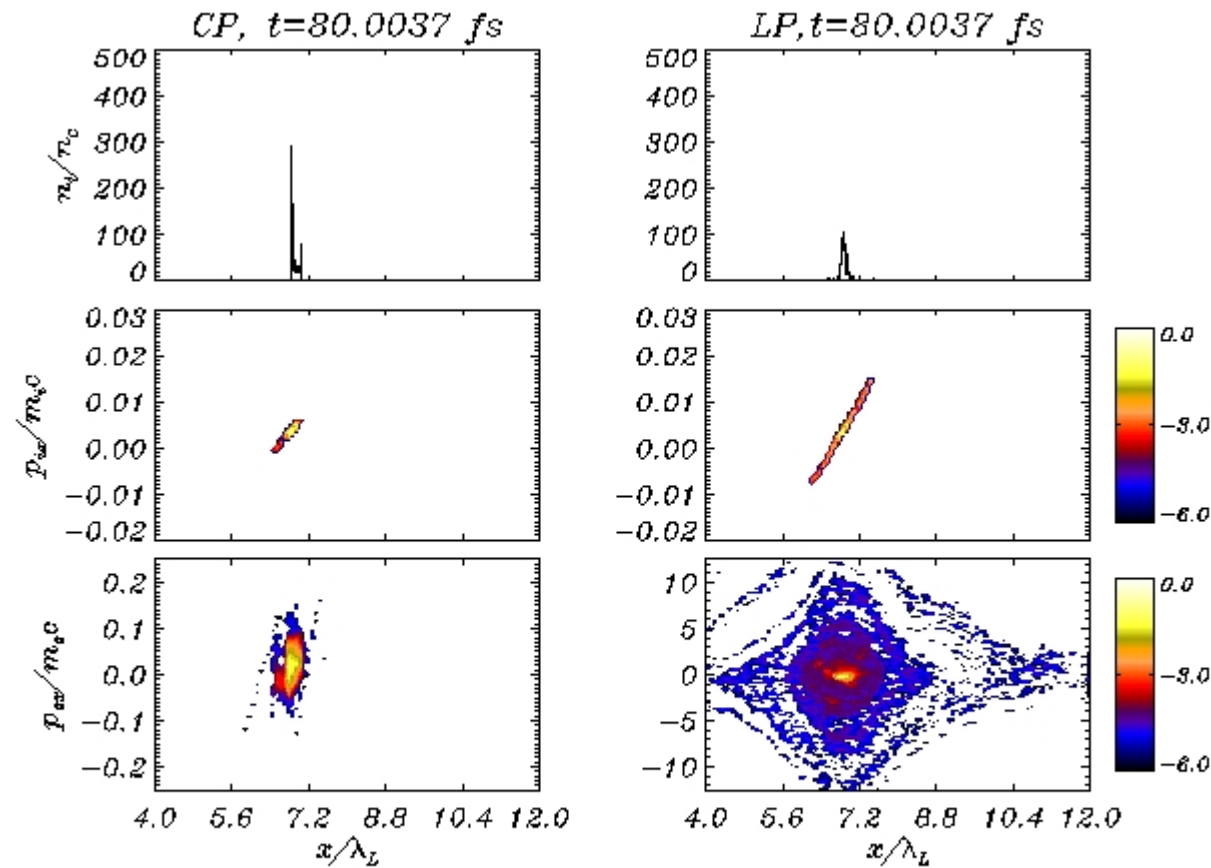
Simulation of thin foil RPA with FLAME parameters

- Carbon target, thickness $d=0.04\mu\text{m}$, $n_e = 250n_c = 4.3 \times 10^{23} \text{ cm}^{-3}$
- Laser: 26 fs pulse, average intensity $I=1.8 \times 10^{20} \text{ W/cm}^2$
relativistic amplitude $a_0 = 13$
- comparison of Linear Polarization vs Circular Polarization case



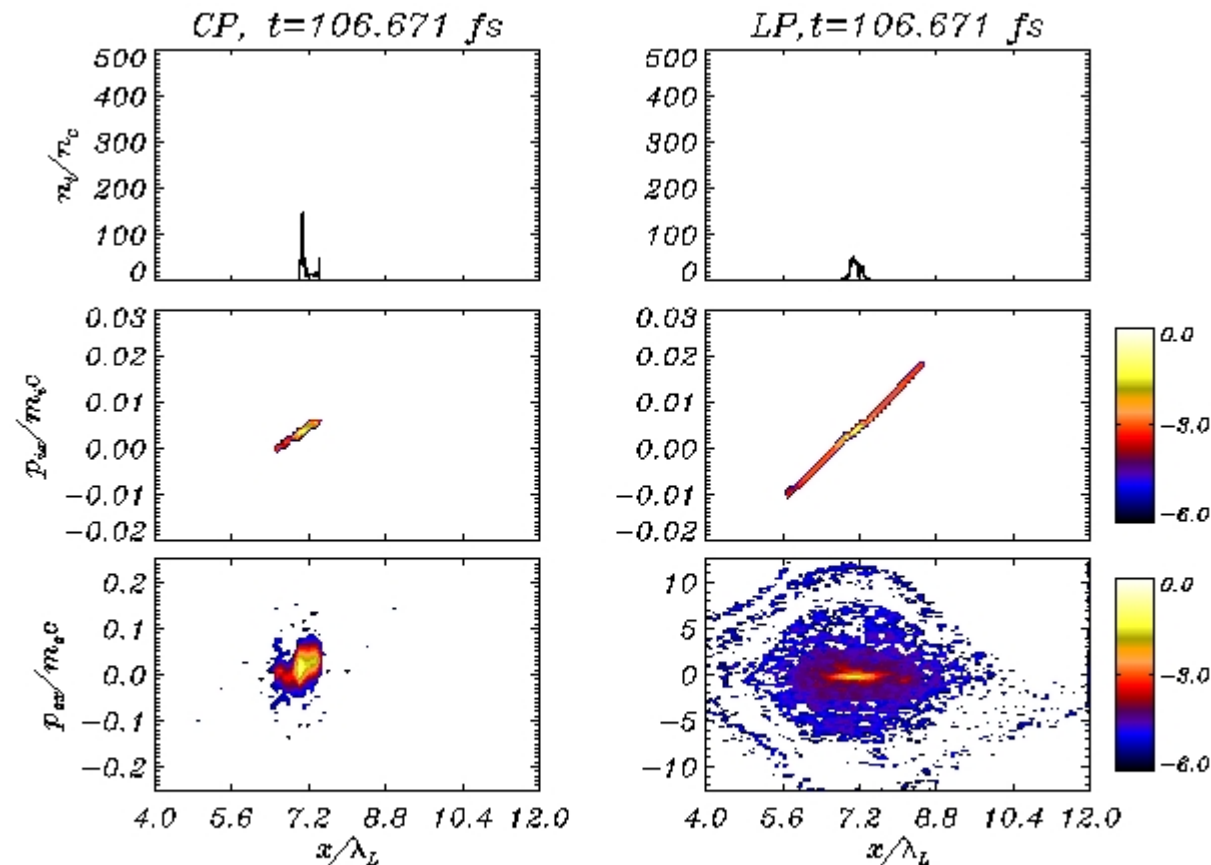
Simulation of thin foil RPA with FLAME parameters

- Carbon target, thickness $d=0.04\mu\text{m}$, $n_e = 250n_c = 4.3 \times 10^{23} \text{ cm}^{-3}$
- Laser: 26 fs pulse, average intensity $I=1.8 \times 10^{20} \text{ W/cm}^2$
relativistic amplitude $a_0 = 13$
- comparison of Linear Polarization vs Circular Polarization case



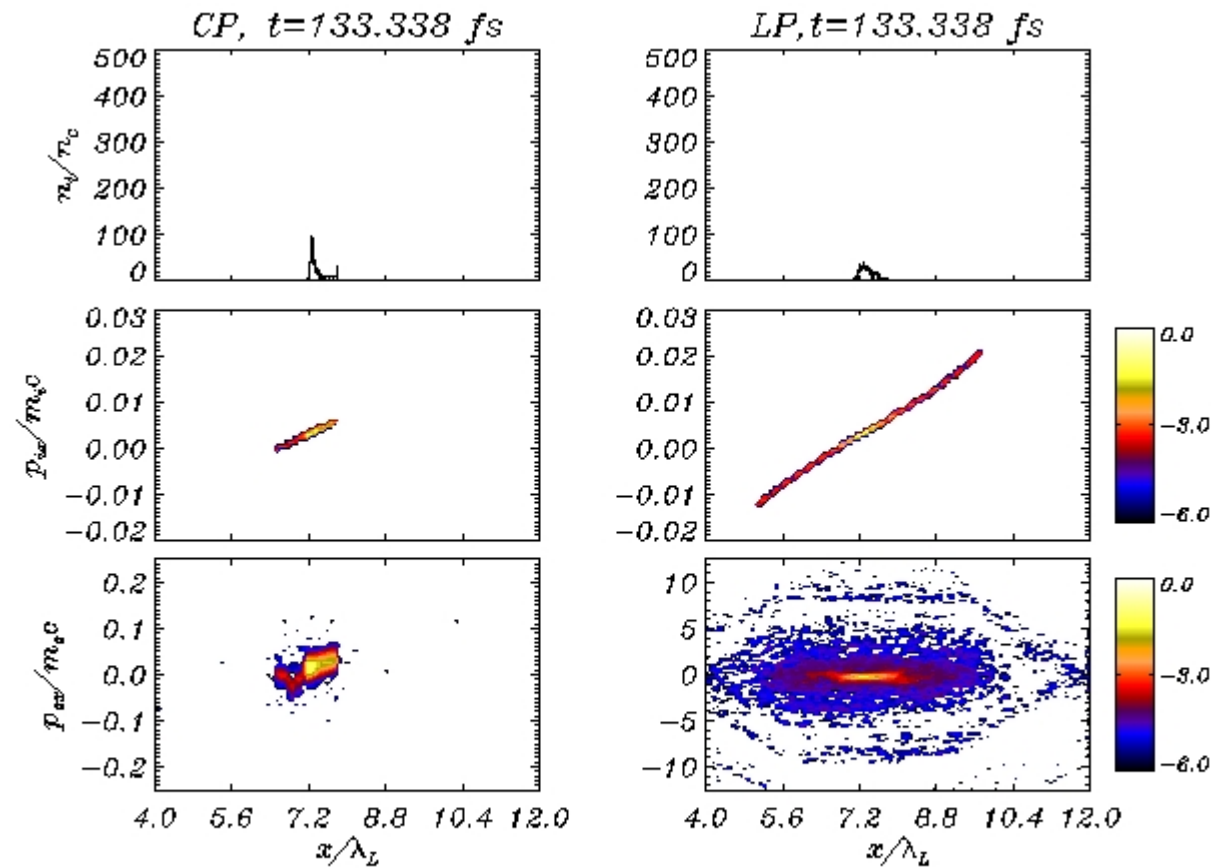
Simulation of thin foil RPA with FLAME parameters

- Carbon target, thickness $d=0.04\mu\text{m}$, $n_e = 250n_c = 4.3 \times 10^{23} \text{ cm}^{-3}$
- Laser: 26 fs pulse, average intensity $I=1.8 \times 10^{20} \text{ W/cm}^2$
relativistic amplitude $a_0 = 13$
- comparison of Linear Polarization vs Circular Polarization case



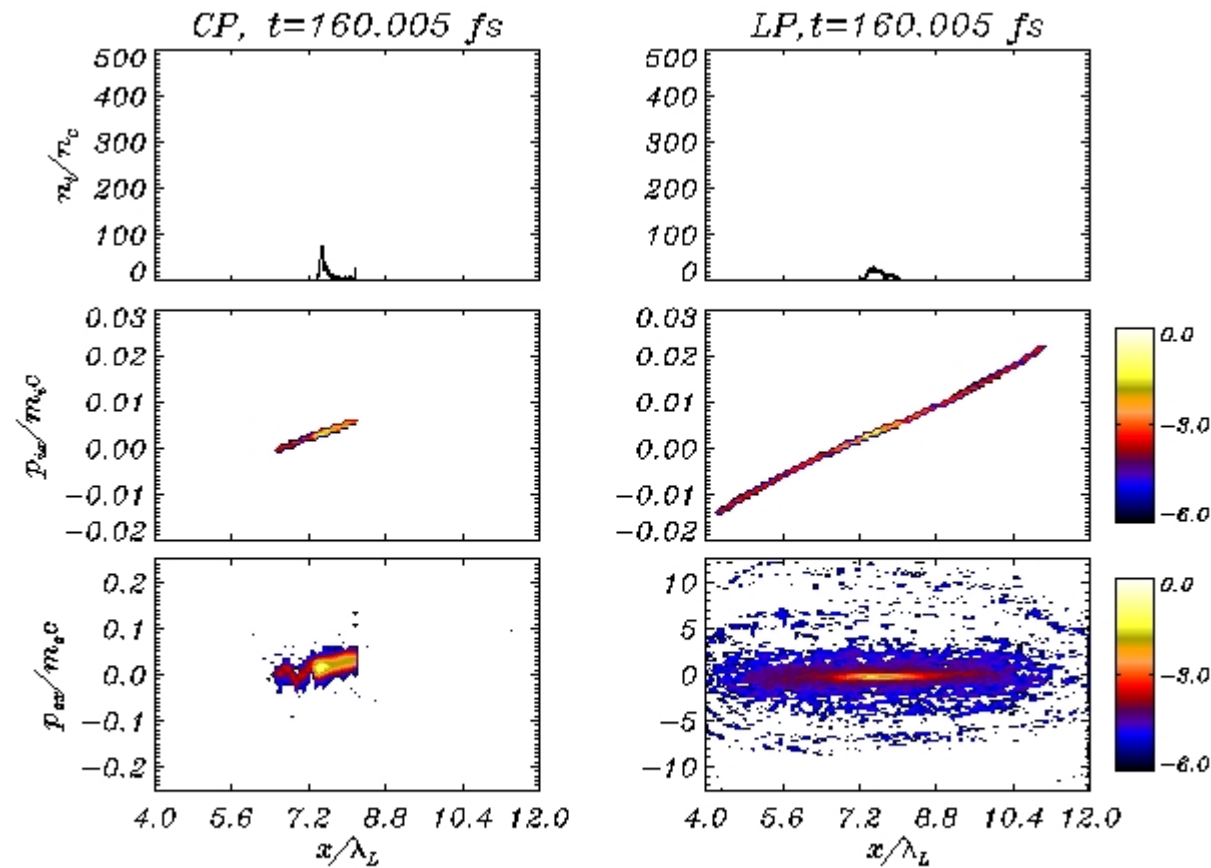
Simulation of thin foil RPA with FLAME parameters

- Carbon target, thickness $d=0.04\mu\text{m}$, $n_e = 250n_c = 4.3 \times 10^{23} \text{ cm}^{-3}$
- Laser: 26 fs pulse, average intensity $I=1.8 \times 10^{20} \text{ W/cm}^2$
relativistic amplitude $a_0 = 13$
- comparison of Linear Polarization vs Circular Polarization case



Simulation of thin foil RPA with FLAME parameters

- Carbon target, thickness $d=0.04\mu\text{m}$, $n_e = 250n_c = 4.3 \times 10^{23} \text{ cm}^{-3}$
- Laser: 26 fs pulse, average intensity $I=1.8 \times 10^{20} \text{ W/cm}^2$
relativistic amplitude $a_0 = 13$
- comparison of Linear Polarization vs Circular Polarization case

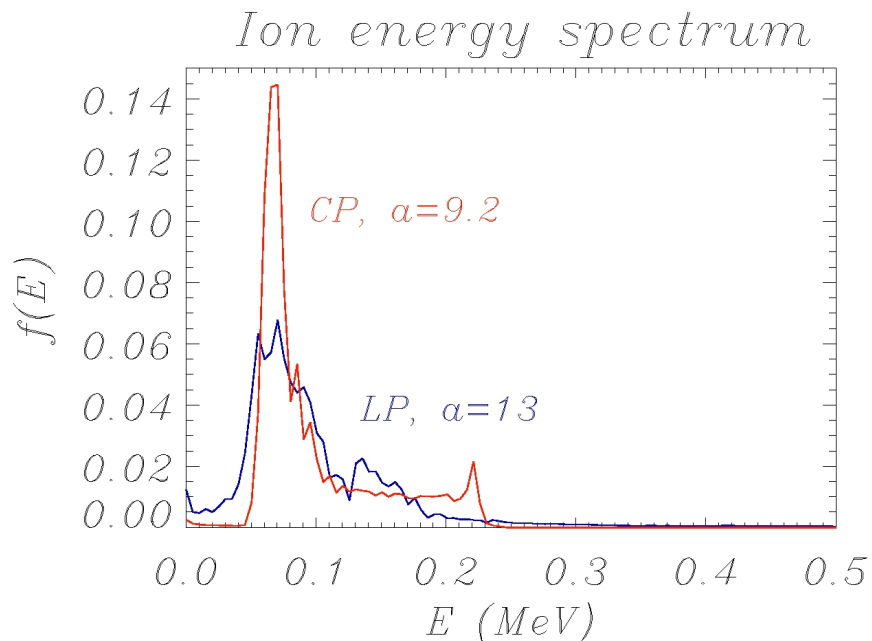


Simulation of thin foil RPA with FLAME parameters

- Carbon target, thickness $d=0.04\mu\text{m}$, $n_e = 250n_c = 4.3 \times 10^{23} \text{ cm}^{-3}$
- Laser: 26 fs pulse, average intensity $I=1.8 \times 10^{20} \text{ W/cm}^2$

relativistic amplitude $a_0 = 13$

- comparison of Linear Polarization vs Circular Polarization case



similarity of spectra suggest relatively weak differences between CP and LP:

- RPA already dominant?
 - optimal thicknesses for acceleration?
- Regime may be quite different with preplasma (thicker targets)

Conclusions

- So far experiments on ion (proton) acceleration from solid targets are dominated by the TNSA mechanism
- Present regimes may approach the transition to the Radiation Pressure Acceleration regimes
- Use of circular polarization enforces the RPA dominance
- Proof of principle of RPA on thin foils may be obtained in present-day laser facilities, including FLAME

This talk may be downloaded from

www.df.unipi.it/~macchi/talks.html

Basis of theoretical and numerical modeling

“Plasma physics is just waiting for bigger computers”

Vlasov-Maxwell
system for
collisionless,
classical plasmas:
kinetic equations are
coupled to EM fields

$$\frac{df_a}{dt}(\mathbf{x}, \mathbf{p}, t) = \frac{\partial f_a}{\partial t} + \dot{\mathbf{x}}_a \frac{\partial f_a}{\partial \mathbf{x}} + \dot{\mathbf{p}}_a \frac{\partial f_a}{\partial \mathbf{p}} = 0, \quad a = (e, i)$$

$$\dot{\mathbf{p}}_a = q_a(\mathbf{E} + \mathbf{v} \times \mathbf{B}), \quad \dot{\mathbf{x}}_a = \frac{\mathbf{p}_a}{m_a \gamma_a},$$

$$\rho(\mathbf{x}, t) = \sum_{a=e,i} q_a \int d^3p f_a, \quad \mathbf{J}(\mathbf{x}, t) = \sum_{a=e,i} q_a \int d^3p \mathbf{v} f_a,$$

$$\nabla \cdot \mathbf{E} = \rho, \quad \nabla \cdot \mathbf{B} = 0, \quad \nabla \times \mathbf{E} = -\partial_t \mathbf{B}, \quad \nabla \times \mathbf{B} = \mathbf{J} + \partial_t \mathbf{E}$$

Mostly used numerical approach: **particle-in-cell** (PIC) method
[Birdsall & Langdon, *Plasma Physics via Computer Simulation* (IOP, 1991)]

3D numerical simulations of “realistic” experimental conditions
is most of the times **beyond present-day supercomputing power**

Models are needed to interpretate experiments and unfold the
underlying physics